

MASTER

Theoretical analysis of squeeze films

Op den Camp, O.M.G.C.

Award date:
1991

[Link to publication](#)

Disclaimer

This document contains a student thesis (bachelor's or master's), as authored by a student at Eindhoven University of Technology. Student theses are made available in the TU/e repository upon obtaining the required degree. The grade received is not published on the document as presented in the repository. The required complexity or quality of research of student theses may vary by program, and the required minimum study period may vary in duration.

General rights

Copyright and moral rights for the publications made accessible in the public portal are retained by the authors and/or other copyright owners and it is a condition of accessing publications that users recognise and abide by the legal requirements associated with these rights.

- Users may download and print one copy of any publication from the public portal for the purpose of private study or research.
- You may not further distribute the material or use it for any profit-making activity or commercial gain

Theoretical analysis of squeeze films

Olaf op den Camp

eindstudiedocent : prof.dr.ir. J.D. Janssen
begeleiding : dr.ir. C.W.J. Oomens
ir. M.A.M. v. Lankveld

Eindhoven, augustus 1991

Technische Universiteit Eindhoven

Faculteit Werktuigbouwkunde

Vakgroep Fundamentele Werktuigkunde W.F.W, 91.063

Summary

The objective of this report is to increase the insight into squeeze film lubrication. This lubrication mechanism is supposed to be responsible for the excellent friction characteristics of the knee-joint. It is based upon the principle, that in a viscous fluid film, which is forced out from between a pair of normally approaching surfaces, pressures are developed, which resist the tendency of the surfaces to come together.

Three special squeeze films have been investigated, i.e. a squeeze film between :

1. two rigid impermeable approaching flat circular plates
2. a rigid impermeable spherical indenter approaching an impermeable rigid flat plate
3. a rigid impermeable circular flat plate approaching a rigid permeable biphasic fluid-solid mixture

For each case the thickness of the squeeze film as a function of time and the pressure distribution over the squeeze film are calculated, given a prescribed load on the upper plate or indenter. By comparing the second with the first case, the pressure distribution appears to be remarkably affected by the geometry of the squeeze film. Moreover the squeeze film lasts much shorter in the second than in the first case.

In the third case interaction between the viscous squeeze film and the viscous interstitial fluid of the mixture has been achieved by using the interface boundary conditions according to Hou (1989). For this case parameters are defined to characterize a mixture. The influence of the presence of a mixture has been clearly demonstrated by comparing the film thickness as a function of time for several combinations of parameters.

It will be valuable to validate Hou's interface conditions by experiments on a physical squeeze film model, which incorporates a rigid mixture.

Contents

Summary	3
Nomenclature	7
1. Introduction	13
2. A squeeze film between a spherical indenter and a cartilage layer	17
2.1. Introduction	17
2.2. Equations of motion for the fluid film	19
2.3. Equations of motion for the cartilage layer	22
2.3.1. Cartilage as a solid-fluid biphasic mixture	22
2.3.2. Constitutive relations for the mixture	24
2.3.3. Equations of motion	28
2.4. Boundary conditions	30
2.4.1. The indenter - fluid film interface	30
2.4.2. The fluid film - mixture interface	30
2.4.3. The mixture - subchondral bone interface	32
2.4.4. Additional boundary conditions	33
2.5. Summary of equations and boundary conditions	34
3. Solution of the equations of motion for three special cases	37
3.1. Introduction	37
3.2. Two rigid impermeable parallel approaching plates	38
3.2.1. Problem definition	38
3.2.2. Simplification of the equations of motion using power series expansions	39
3.2.3. Film thickness and pressure distribution over the squeeze film	43

3.3.	A rigid impermeable spherical indenter approaching a rigid impermeable plane	49
3.3.1.	Problem definition	49
3.3.2.	Film thickness and pressure distribution over the squeeze film	50
3.4.	A rigid impermeable circular plate approaching a rigid permeable biphasic fluid-solid mixture	57
3.4.1.	Problem definition	57
3.4.2.	Equations of motion for the fluid film	58
3.4.3.	Equations of motion for the biphasic mixture	60
3.4.4.	Film thickness and pressure distribution over the squeeze film	68
3.4.5.	Results	70
4.	Conclusions and recommendations	77
	References	79
	Appendix I	81
	I.1. Vector identities in Cartesian coordinates	81
	I.2. Vector identities in cylindrical coordinates	83
	Appendix II	85
	II.1. Program to generate an input file	85
	II.2. Programs to calculate the squeeze film thickness	89
	II.2.1. Two plates	89
	II.2.2. Spherical indenter - Plate	93
	II.2.3. Plate - Mixture	97
	Appendix III Constraints on the constitutive relations for the mixture	103
	Samenvatting	109

Nomenclature

c^α	mass supply to α^{th} phase from other constituents	[kg m ⁻³ s ⁻¹]
$F(t)$	load on upper plate/indenter in z-direction	[N]
F_0	load scaling factor	[N]
g	surface position of indenter in squeeze action	[m]
H_A	= $\lambda_s + 2\mu_s$ = rigidity of solid matrix	[N m ⁻²]
H_0	initial thickness of cartilage layer/mixture	[m]
h	squeeze film thickness	[m]
h_0	initial squeeze film thickness	[m]
\vec{h}^α	heatflux vector	[J m ⁻² s ⁻¹]
K	dragcoefficient = $(n^f)^2 / k$	[N s m ⁻⁴]
k	permeability	[m ⁴ N ⁻¹ s ⁻¹]
m	total mixture mass	[kg]
m^α	mass of α^{th} phase	[kg]
n^α	partial volume fraction of α^{th} phase	[-]
p	pressure	[N m ⁻²]
P_0	pressure scaling factor	[N m ⁻²]
\vec{q}^α	external body force per unit mass	[N m ⁻³ kg ⁻¹]
R_i	radius of spherical indenter	[m]
R_0	radial dimensional scaling factor (characteristic radius of load carrying area)	[m]
r	radial coordinate	[m]
t	time	[s]
t_0	time scaling factor	[s]
$\vec{\tau}^\alpha$	force per unit area that α^{th} phase outside a certain volume element exerts on α inside this volume element	[N m ⁻²]
\vec{u}	displacement of solid matrix	[m]
(u_r, u_ϕ, u_z)	displacement coordinates	[m]
$V(t)$	upper plate/indenter velocity in squeeze action	[m s ⁻¹]
V_0	velocity scaling factor in z-direction	[m s ⁻¹]
V	mixture volume	[m ³]

V^α	volume of α^{th} phase	[m ³]
\vec{v}	velocity vector	[m s ⁻¹]
(v_r, v_φ, v_z)	velocity components	[m s ⁻¹]
v_{rh}	radial fluid velocity at fluid mixture interface	[m s ⁻¹]
v_{zh}	axial fluid velocity at fluid mixture interface	[m s ⁻¹]
z	axial coordinate	[m]
α	ratio of h_0 and R_0	[-]
β	ratio of h_0 and H_0	[-]
δ	parameter = $\sqrt{\eta_a/(KH_0^2)}$	[-]
η	parameter = $(n^f)^2 \eta_f / \eta_a$	[-]
η^α	specific entropy	[J kg ⁻¹ K ⁻¹]
η_a	apparent viscosity of fluid phase	[N s m ⁻²]
η_f	viscosity of single phase fluid	[N s m ⁻²]
θ^α	absolute temperature	[K]
λ	Lagrange multiplier	[N m ⁻²]
λ_s	Lamé constants of solid matrix	[N m ⁻²]
$\vec{\pi}^\alpha$	body force due to interaction with other components	[N m ⁻³]
ρ	mixture density	[kg m ⁻³]
ρ^α	apparent density of α^{th} phase	[kg m ⁻³]
$\rho^{\alpha*}$	true density of α^{th} phase	[kg m ⁻³]
φ	tangential coordinate	[-]
ϕ^α	specific internal energy	[J kg ⁻¹]
ψ^α	specific Helmholtz free energy	[J kg ⁻¹]
$\vec{\nabla}$	gradient vector	[m ⁻¹]

indices

α, s, f	α^{th} phase, solid, fluid
c	conjugate
r, φ, z	r, φ, z direction
$+$	fluid side of fluid mixture interface
$-$	mixture side of fluid mixture interface
0	undeformed state

tensors

D	rate of deformation tensor	[s ⁻¹]
E	Green-Lagrange strain tensor	[-]
ϵ	linear strain tensor	[-]
F	deformation tensor	[-]
I	unit second order tensor	[-]
P	2 ^{de} Piola-Kirchhoff stress tensor	[N m ⁻²]
σ	Gauchy stress tensor	[N m ⁻²]

When a film of viscous fluid is forced out from between a pair of approaching surfaces, pressures are developed which resist the tendency of the surfaces to come together. Under such conditions the fluid layer is described as a squeeze film.

(O'Connor and Boyd, 1968)

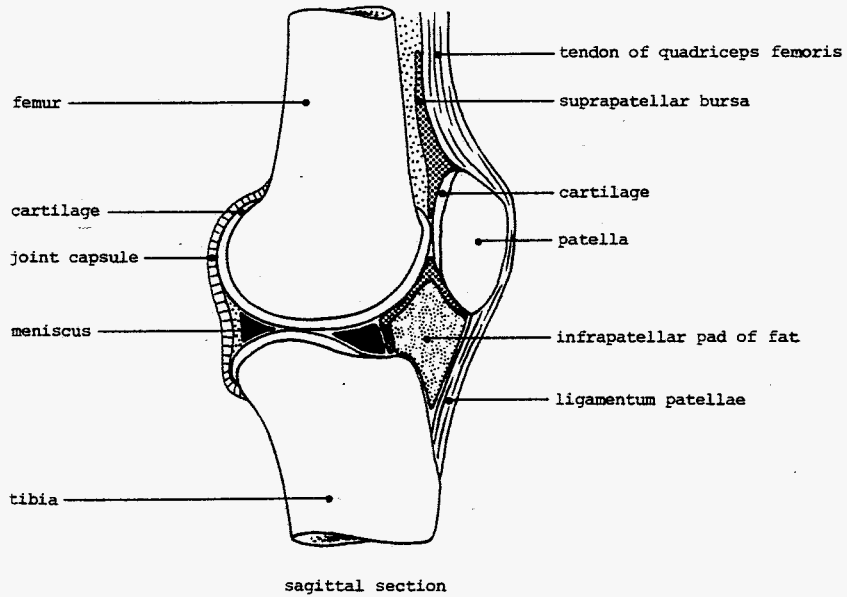
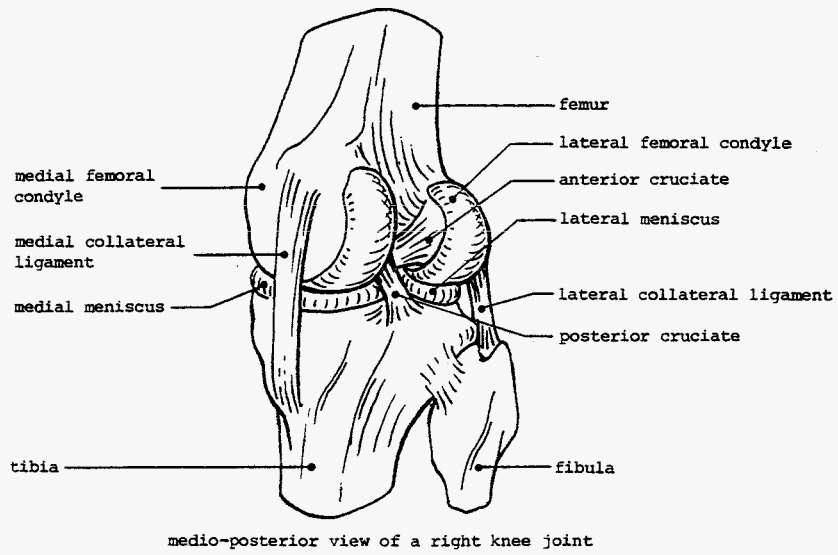


figure 1 *The human knee-joint (Wismans, 1980)*

Chapter 1. Introduction

The knee-joint (figure 1) ensures nearly frictionless motions of the shinbone (tibia) relative to the thighbone (femur) (McCutchen, 1978). It is generally believed that operation of the knee is due to the structure of the joint. However, insight into the mechanical behaviour of the knee-joint is still limited.

Major components in the joint are the synovial lubricating fluid, and the cartilage layers which cover the two articular bone surfaces. Moreover, menisci, ligaments, joint-capsule, muscles etc. can be distinguished. The menisci, two semi-circular disks with wedge-shaped cross-sections fill the space in between the two incongruent articular surfaces. The joint-capsule and the ligaments connect femur and tibia. The lining membrane of the joint-capsule synovia is believed to secrete and maintain the synovial fluid (Mow, 1969).

Recently a theoretical model has been developed by Schreppers (1991), focused on the force transmission through the knee-joint. Because the complete knee-joint is a very complex load transmitting connection, a modeling strategy, which is characterized by a stepwise approach, has been presented. First Schreppers distinguished three interacting sub-connections in the knee, i.e.:

- capsule and ligaments
- muscles, tendons, and related fibrous sheets
- the contact between the cartilage layers, directly as well as indirectly via both the menisci and the synovial fluid.

Before these sub-connections can be integrated into a model of the complete knee-joint, insight into the distinct sub-connections has to be obtained.

In his report Schreppers focused on the third subconnection, which provides load transmission via the contact between the cartilage layers (figure 2). He presented an axi-symmetric model which contains a planar disk, representing an articular cartilage layer, a spherical indenter and, in between, a toroid with a wedge-shaped cross-section, representing the meniscus. The lower end plane of the articular layer is fixed to a rigid support. The synovial fluid is enclosed in the resulting cavity between the indenter, the meniscus, and the cartilage layer. Frictionless sliding of the meniscal ring along the articular cartilage layer and the spherical indenter as well as sliding of the articular cartilage layer along the spherical indenter is allowed. The articular cartilage layer as well as the meniscus are considered to be mixtures of a purely elastic homogeneous solid and an ideal fluid. The synovial fluid is also considered as an ideal fluid.

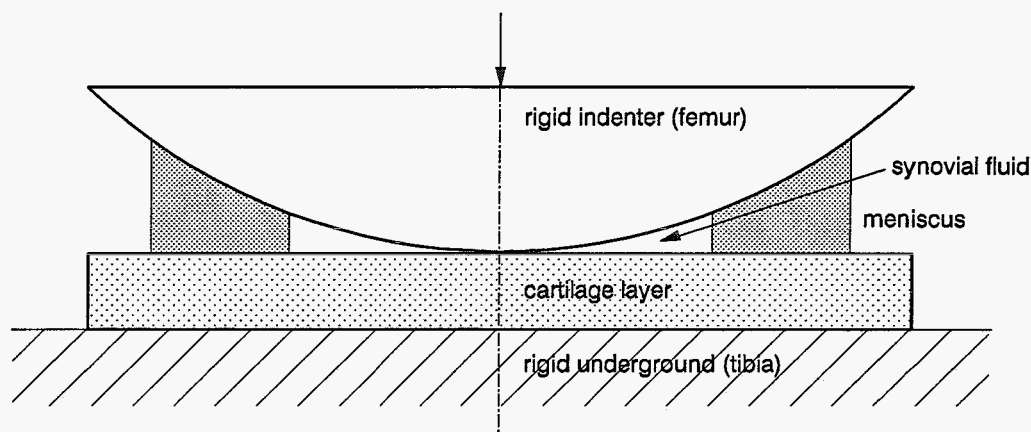


figure 2 Cross-section of the axisymmetric model of the load transmitting contact between the cartilage layers (Schreppers, 1991).

From the numerical analyses based on this model (using the finite element method) the interaction between the components appeared to be an important aspect of the load transmission in the knee joint.

Schreppers (1991) recommended to continue with a stepwise development of the model described above. Attention should be focused on the interaction between a mixture and its surrounding fluid as well as between mixtures mutually. Following this strategy, it may become possible to include the viscosity of both the synovial fluid and the interstitial fluid into the model.

For the last decades researchers have investigated interaction effects between the synovial fluid and articular cartilage, in order to explain the excellent friction characteristics of the knee-joint. As a result many lubrication mechanisms have been proposed for this joint. Hou (1989) mentioned the most important among them, such as wedge-film hydrodynamic lubrication, elasto-hydrodynamic lubrication, squeeze film lubrication, weeping lubrication, and boosted lubrication. Each of these mechanisms will be explained briefly.

In hydrodynamic lubrication the shape and relative motion of rigid sliding surfaces cause the formation of a wedge-shaped fluid film, having sufficient pressure to separate the surfaces (O'Connor and Boyd, 1968). If the deformation of the cartilage is taken into account, the mechanism is known as elasto-hydrodynamic lubrication. However both lubrication modes require a fast relative tangential motion between the two joint surfaces. This is not the case for the knee-joint, where high compressive loading stresses are combined with a low operating speed (Mow, 1969).

For squeeze film lubrication only normal surface motions are required. Squeeze film lubrication is based upon the principle, that in a fluid film, which is forced out from between a pair of normally approaching surfaces, pressures are developed, which resist the tendency of the surfaces to come together (O'Connor and Boyd, 1968).

Alternative squeeze film mechanisms deal with the porous-permeable and deformable nature of cartilage. 'Weeping lubrication' is a so called self-pressurized hydrostatic lubrication mechanism (McCutchen, 1978). The lubricating fluid film is assumed to be supplied by the interstitial fluid which is squeezed out from the cartilage by compressing the cartilage.

Finally Hou (1989) mentioned an alternative theory called 'Boosted lubrication', where the synovial fluid flows into the cartilage layer during squeeze action. However the large molecules in the synovial fluid are not able to penetrate the cartilage, resulting in a concentrated solution with high viscosity in the joint gap (Lai, 1978), which lubricates the articulating surfaces.

For the squeeze film mechanism in the knee-joint, many mathematical analyses have been presented. Solutions of these analyses however highly depend on the various imposed boundary conditions (Hou, 1989). Thus, investigating interaction effects requires proper boundary conditions at the interface between mixtures or between a mixture and a viscous fluid.

Hou (1989) proposed the 'pseudo-no-slip' condition, based upon the principle that the conditions at the interface between mixtures or between mixtures and fluids must reduce to those boundary conditions in single phase continuum mechanics. From this proposed kinematic boundary condition, and balance of mass, momentum, and energy, the required boundary conditions at the interface between a biphasic mixture and a Newtonian fluid are mathematically derived.

With these interface boundary conditions, Hou is capable to model the squeeze film mechanism in the tibio-femoral joint. This model is axi-symmetric. A rigid and impermeable underground is covered by a deformable permeable layer, representing the cartilage. The gap between the surface of the layer and a rigid impermeable spherical indenter contains a viscous fluid. No meniscus is incorporated into the model. Hou performs the analyses of the model almost fully analytically. Hou concluded that if the joint is loaded with a compressive force, the cartilage layers deform to form a pair of mating surfaces, more congruent than in the unloaded state, resulting in a spread of the load to a larger area. When the joint gap becomes very thin, the synovial fluid flows into the cartilage at the central region of the joint, which makes 'boosted lubrication' likely to occur.

The objective of this study is to increase the insight into squeeze film lubrication by means of the analysis of three special cases of Hou's model, i.e.:

- Two rigid impermeable approaching circular plates,
- A rigid impermeable spherical indenter approaching an impermeable rigid plane,
- A rigid impermeable circular plate approaching a rigid permeable biphasic fluid-solid mixture.

Moreover, by working out the third case, where a mixture is incorporated, it may become possible in the future to verify the interface conditions experimentally.

In chapter 2 the governing equations for the squeeze film model (Hou, 1989) are derived using the balance of mass and momentum, the theory of mixtures, and the interface boundary conditions according to Hou. In chapter 3 these general equations are simplified using power series expansions. For each case the film thickness as a function of time will be calculated, given the prescribed load on the upper plate or indenter. In chapter 4 conclusions and recommendations will be given in consequence of the results in chapter 3.

Chapter 2. A squeeze film between a spherical indenter and a cartilage layer

2.1. Introduction

To investigate the lubrication mechanism of the human knee-joint, a squeeze film model may be used, in which the interaction between the synovial fluid and the cartilage layer is taken into account. Squeeze film lubrication is based upon the principle, that in a fluid film, which is forced out from between a pair of approaching surfaces, pressures are developed, which resist the tendency of the surfaces to come together. The squeeze film model, which will be described in this chapter, has a rotationally symmetric, simple geometry (figure 3) :

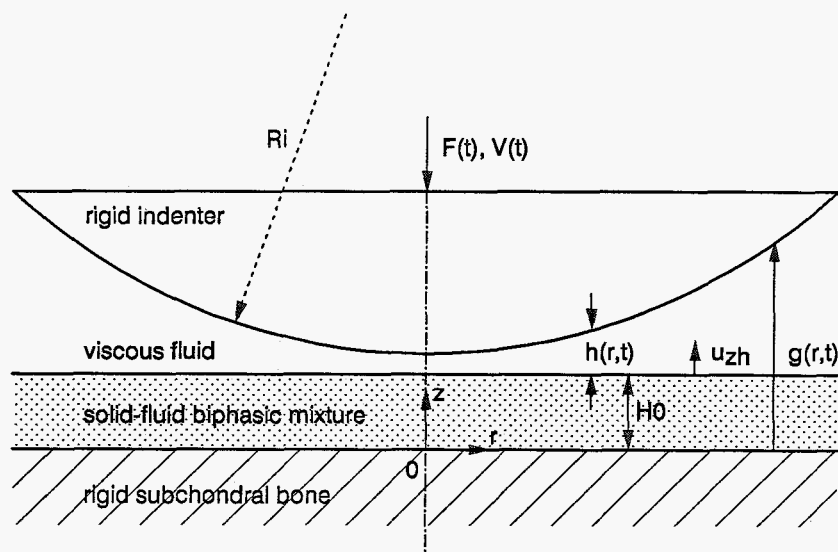


figure 3 Schematic diagram of a squeeze film between a rigid indenter and a cartilage layer. Symbols will be explained in the text.

The rigid and impermeable subchondral bone is covered by a thin layer of cartilage with thickness H_0 . Within the gap between the spherical indenter with radius R_i and the cartilage layer an incompressible Newtonian fluid with viscosity η_f is found. The indenter is subjected to a prescribed load $F(t)$ in the negative z -direction. As a result of the indenter load, the indenter moves in the negative z -direction with a velocity $V(t)$. The distances $h(r,t)$, u_{zh} and $g(r,t)$ denote the film thickness, the axial deformation of the cartilage surface, and the position of the indenter surface respectively.

The cartilage is assumed to be a mixture of an elastic solid and a viscous fluid, which are homogeneously distributed over the whole mixture volume, while both continua follow their own motion. The model assumes Newtonian behaviour of the synovial fluid and isotropic linear elastic behaviour of the solid matrix, while the constitutive laws under consideration are based on finite deformations. The equations of motion are formulated for each constituent separately, but they are coupled because each position in the mixture is occupied by fluid as well as by solid. Moreover, the constituents may interact both mechanically and chemically (Oomens 1985, page 3.5).

A fixed coordinate system is defined in space with origin O , axial coordinate z , radial coordinate r , and tangential coordinate φ . Since the model is axi-symmetric, the solid displacement and the fluid velocity in the tangential direction are equal to 0. Moreover the derivatives with respect to φ are equal to 0.

2.2. Equations of motion for the fluid film

The motion of the fluid film is governed by the laws of conservation of mass, momentum and moment of momentum. The balance of mass for a fluid with density ρ^f is given by :

$$\frac{\partial \rho^f}{\partial t} + \vec{\nabla} \cdot (\rho^f \vec{v}^f) = 0 \quad (2.1)$$

where t , $\vec{\nabla}$, and \vec{v}^f denote the time, the gradient vector and the fluid velocity vector respectively.

The balance of momentum is :

$$\rho^f \left(\frac{\partial \vec{v}^f}{\partial t} + \vec{v}^f \cdot \vec{\nabla} \vec{v}^f \right) = \vec{\nabla} \cdot (\sigma^f)^c + \rho^f \vec{q}^f \quad (2.2)$$

where $(\sigma^f)^c$ is the conjugate of the fluid stress tensor and \vec{q}^f is the external body force. This equation states that the change of momentum with time is equal to the sum of surface and body forces.

The following assumptions are made to elaborate the equations of motion :

assumption 1 Both unsteady and convective inertia forces will be neglected :

$$\frac{\partial \vec{v}^f}{\partial t} + \vec{v}^f \cdot \vec{\nabla} \vec{v}^f = \vec{\delta} \quad (2.3)$$

assumption 2 Body forces will be neglected :

$$\vec{q}^f = \vec{\delta} \quad (2.4)$$

assumption 3 Conservation of moment of momentum means :

$$(\sigma^f)^c = \sigma^f \quad (2.5)$$

assumption 4 The fluid is assumed to be incompressible (the density ρ^f is constant) :

$$\frac{\partial \rho^f}{\partial t} = 0, \quad \vec{\nabla} \rho^f = \vec{\delta} \quad (2.6)$$

assumption 5 The fluid is assumed to be Newtonian with viscosity η_f , so the constitutive model reads :

$$\sigma^f = -pI + 2\eta_f D^f \quad \text{with:} \quad D^f = \frac{1}{2}((\nabla \cdot \vec{v}^f)^c + (\nabla \vec{v}^f)) \quad (2.7)$$

so the fluid stress tensor is split into a term due to the pressure and a term due to the shear loadings. D^f is the rate of deformation tensor.

The balance laws may thus be rewritten as :

$$\begin{aligned} \text{conservation of mass :} \quad & \nabla \cdot \vec{v}^f = 0 \\ \text{conservation of momentum :} \quad & \nabla \cdot \sigma^f = \vec{\delta} \end{aligned} \quad (2.8)$$

Using equation (I.11) (Appendix I), the balance of mass for this cylinder-symmetrical problem is represented by :

$$\nabla \cdot \vec{v}^f = \frac{1}{r} \frac{\partial(rv_r^f)}{\partial r} + \frac{\partial v_z^f}{\partial z} = 0 \quad (2.9)$$

The balance of momentum will be rewritten as follows :

$$\begin{aligned} \nabla \cdot \sigma^f &= -\nabla \cdot pI + \eta_f \nabla \cdot ((\nabla \vec{v}^f)^c + (\nabla \vec{v}^f)) \\ &= -\nabla p + \eta_f (\nabla \cdot (\vec{v}^f \nabla) + \nabla \cdot (\nabla \vec{v}^f)) \\ &= -\nabla p + \eta_f ((\nabla \cdot \vec{v}^f) \nabla + \nabla \cdot (\nabla \vec{v}^f)) \\ &= -\nabla p + \eta_f \nabla \cdot (\nabla \vec{v}^f) \\ &= \vec{\delta} \end{aligned} \quad (2.10)$$

where the balance of mass (2.9) is substituted during the last step.

Representing equation (2.10) in coordinates yields :

$$\begin{aligned} -\frac{\partial p}{\partial r} + \eta_f \frac{\partial}{\partial r} \left(\frac{\partial v_r^f}{\partial r} + \frac{v_r^f}{r} \right) + \eta_f \frac{\partial^2 v_r^f}{\partial z^2} &= 0 \\ -\frac{\partial p}{\partial z} + \eta_f \frac{1}{r} \frac{\partial}{\partial r} \left(r \frac{\partial v_z^f}{\partial r} \right) + \eta_f \frac{\partial^2 v_z^f}{\partial z^2} &= 0 \end{aligned} \quad (2.11)$$

Since the problem is cylinder-symmetrical no derivatives with respect to the angle φ are found in the last equation.

2.3. Equations of motion for the cartilage layer

2.3.1. Cartilage as a solid-fluid biphasic mixture

Cartilage is modeled as a biphasic mixture, consisting of a fluid phase f and a solid phase s. The true density ρ_*^α of a phase α (either s or f) is defined as the ratio of the mass m_α of the α^{th} phase and the volume V_α of the α^{th} phase :

$$\rho_*^\alpha = \frac{m^\alpha}{V^\alpha} \quad (2.12)$$

The volume fraction n^α of a phase α is defined as the ratio of the volume of the α^{th} phase and the total mixture volume V :

$$n^\alpha = \frac{V^\alpha}{V} \quad (2.13)$$

One can easily see that :

$$\sum_\alpha n^\alpha = 1 \quad (2.14)$$

The apparent density ρ^α of a phase α is defined as the ratio of the mass of the α^{th} phase and the total mixture volume :

$$\rho^\alpha = \frac{m^\alpha}{V} = n^\alpha \rho_*^\alpha \quad (2.15)$$

The balance equations of mass for the mixture components read (Oomens 1985, page 3.9) :

$$\begin{aligned} \frac{\partial \rho^s}{\partial t} + \vec{\nabla} \cdot (\rho^s \vec{v}^s) &= c^s \\ \frac{\partial \rho^f}{\partial t} + \vec{\nabla} \cdot (\rho^f \vec{v}^f) &= c^f \end{aligned} \quad (2.16)$$

These mass balances deviate from the standard mass balance (2.1) by an interaction term c^α representing the mass supply to the α^{th} phase from the other constituents.

The balance equations of momentum for the mixture components read (Oomens 1985, 3.13) :

$$\begin{aligned} \rho^s \left(\frac{\partial \vec{v}^s}{\partial t} + \vec{v}^s \cdot \vec{\nabla} \vec{v}^s \right) &= \vec{\nabla} \cdot \sigma^s + \rho^s \vec{q}^s + \vec{\pi}^s \\ \rho^f \left(\frac{\partial \vec{v}^f}{\partial t} + \vec{v}^f \cdot \vec{\nabla} \vec{v}^f \right) &= \vec{\nabla} \cdot \sigma^f + \rho^f \vec{q}^f + \vec{\pi}^f \end{aligned} \quad (2.17)$$

which deviate from the standard balance of momentum (2.2) by a vector $\bar{\pi}^\alpha$ representing the body force due to interaction effects with other constituents. For a solid-fluid biphasic mixture these body forces satisfy :

$$\bar{\pi}^s + \bar{\pi}^f = \bar{0}, \quad \bar{\pi}^s = -\bar{\pi}^f \quad (2.18)$$

The following assumptions are made to elaborate the equations of motion :

assumption 6 Both unsteady and convective inertia forces will be neglected :

$$\frac{\partial \bar{v}^\alpha}{\partial t} + \bar{v}^\alpha \cdot \bar{\nabla} \bar{v}^\alpha = 0 \quad (2.19)$$

assumption 7 Body forces will be neglected :

$$\bar{q}^\alpha = \bar{0} \quad (2.20)$$

assumption 8 Mass exchange due to chemical interactions will be neglected :

$$c^\alpha = 0 \quad (2.21)$$

assumption 9 Both components are assumed to be intrinsically incompressible (ρ_*^α is constant) :

$$\frac{\partial \rho_*^\alpha}{\partial t} = 0, \quad \bar{\nabla} \rho_*^\alpha = \bar{0} \quad (2.22)$$

The conservation laws for the mixture components now reduce to :

<p style="text-align: center;">conservation of mass :</p> $\frac{\partial \mathbf{n}^s}{\partial t} + \bar{\nabla} \cdot (\mathbf{n}^s \bar{v}^s) = 0$ $\frac{\partial \mathbf{n}^f}{\partial t} + \bar{\nabla} \cdot (\mathbf{n}^f \bar{v}^f) = 0$ <p style="text-align: right;">(2.23)</p> <p style="text-align: center;">conservation of momentum :</p> $\bar{\nabla} \cdot \boldsymbol{\sigma}^s + \bar{\pi}^s = \bar{0}$ $\bar{\nabla} \cdot \boldsymbol{\sigma}^f - \bar{\pi}^s = \bar{0}$
--

where (2.15) is used.

For later use it is remarked that addition of the balances of mass (from 2.23) leads to :

$$\vec{\nabla} \cdot ((1 - n^f) \vec{v}^s + n^f \vec{v}^f) = \vec{\nabla} \cdot (n^f (\vec{v}^f - \vec{v}^s)) + \vec{\nabla} \cdot \vec{v}^s = 0 \quad (2.24)$$

2.3.2. Constitutive relations for the mixture

Elaborating conservation of momentum requires constitutive relations for the mixture components and the body forces due to interaction. These relations have to satisfy conservation of mass and the second axiom of thermodynamics. In appendix III satisfying relations are proposed.

solid

The constitutive relation for the solid component of the mixture reads (III.9) :

$$\sigma^s = -p n^s I + \rho^s F \cdot \frac{\partial \psi^s}{\partial E^s} \cdot F^c \quad (2.25)$$

where F , ψ^s , and E^s denote the deformation tensor of the solid, the Helmholtz free energy, and the Green-Lagrange strain tensor respectively. To get a useful expression for this model, a relation for the derivative of the Helmholtz free energy ψ^s with respect to the Green-Lagrange strain tensor E^s has to be found.

The second term at the right hand side of equation (2.25) is known as the effective stress (Oomens 1985, page 3.13):

$$\sigma^{s \text{ eff}} = \rho^s F \cdot \frac{\partial \psi^s}{\partial E^s} \cdot F^c \quad (2.26)$$

The effective stress is the stress required to deform the solid *matrix* (with pores but without the interstitial fluid).

The relation between the Cauchy stress tensor $\sigma^{s \text{ eff}}$ and the second Piola-Kirchhoff effective stress $P^{s \text{ eff}}$ is by definition equal to:

$$\sigma^{s \text{ eff}} = \frac{1}{\det F} F \cdot P^{s \text{ eff}} \cdot F^c = \frac{\rho^r}{\rho_o^r} F \cdot P^{s \text{ eff}} \cdot F^c \quad (2.27)$$

One can easily see from the equations (2.26) and (2.27) that :

$$\frac{\partial \psi^s}{\partial \mathbf{E}^s} = \frac{1}{\rho_0^s} \mathbf{P}^{s \text{ eff}} \quad (2.28)$$

For an isotropic purely elastic material the following linear relation between $\mathbf{P}^{s \text{ eff}}$ and \mathbf{E}^s can be chosen :

$$\mathbf{P}^{s \text{ eff}} = \lambda_s \text{tr}(\mathbf{E}^s) \mathbf{I} + 2\mu_s \mathbf{E}^s \quad (2.29)$$

where λ_s and μ_s are Lamé constants.

This relation between $\mathbf{P}^{s \text{ eff}}$ and \mathbf{E}^s allows compression of the solid matrix.

With (2.28) and (2.29) the constitutive model for the solid matrix (2.25) may be written as :

$$\boldsymbol{\sigma}^s = -p \mathbf{n}^s \mathbf{I} + \frac{1}{\det \mathbf{F}} \mathbf{F} \cdot \{ \lambda_s \text{tr}(\mathbf{E}^s) \mathbf{I} + 2\mu_s \mathbf{E}^s \} \cdot \mathbf{F}^c \quad (2.30)$$

In case of infinitesimal deformations this model becomes :

$$\boldsymbol{\sigma}^s = -p \mathbf{n}^s \mathbf{I} + \lambda_s \text{tr}(\boldsymbol{\varepsilon}) \mathbf{I} + 2\mu_s \boldsymbol{\varepsilon} \quad (2.31)$$

where $\boldsymbol{\varepsilon}$ is the linear strain tensor :

$$\boldsymbol{\varepsilon} = \frac{1}{2} \{ (\nabla \vec{u}) + (\nabla \vec{u})^c \} \quad (2.32)$$

Fluid

The constitutive relation for the fluid component of the mixture (the interstitial fluid) (III.10) reads :

$$\sigma^f = -p_n^f \mathbf{I} + \sigma^{fv} \quad (2.33)$$

where σ^{fv} is the viscous part of the stress tensor σ^f .

For a *compressible Newtonian fluid matrix*, the stress tensor can be given by :

$$\sigma^{fv} = -\frac{2}{3}\eta_a \text{tr}(D^f) \mathbf{I} + 2\eta_a D^f \quad (2.34)$$

where D^f is the rate of deformation tensor :

$$D^f = \frac{1}{2} \{ (\nabla \vec{v}^f) + (\nabla \vec{v}^f)^c \} \quad (2.35)$$

and η_a the apparent viscosity of the interstitial fluid (Hou, 1989).

In consideration of the interaction at the interface between the fluid film and the interstitial fluid, the viscosity of the fluid mixture component has to be taken into account. If the interaction between the interstitial fluid and the surrounding fluid is not as important as other effects like mechanical loading or pressure gradients (e.g. in case of confined compression (Oomens, 1985)), the interstitial fluid may be considered to be inviscous. In those cases however, only the apparent viscosity in the stress tensor is neglected. The dragcoefficient still depends on the viscous nature of the interstitial fluid, because shear stresses can only be exerted on fluids, if they are viscous.

Further, Hou states that the apparent viscosity η_a usually deviates from the fluid film viscosity due to the solid matrix. Values for the apparent viscosity are not currently available. However, it is expected that they range from 10^{-3} to 10 Pa s (Hou 1989, page 83).

Body forces

A linear relation between the body forces due to interaction $\bar{\pi}^s$ and $\bar{\pi}^f$ and the relative velocity of the fluid with respect to the solid ($\bar{v}^f - \bar{v}^s$) is proposed (III.14) :

$$\bar{\pi}^s = \mathbf{K} \cdot (\bar{v}^f - \bar{v}^s) \quad (2.36)$$

where \mathbf{K} is the dragcoefficient. Lai and Mow (1980) gave a relation between the dragcoefficient \mathbf{K} and the permeability k :

$$\mathbf{K} = \frac{(\mathbf{n}^f)^2}{k} \quad (2.37)$$

Summary of the constitutive relations

$$\sigma^s = -p n^s \mathbf{I} + \lambda_s \text{tr}(\boldsymbol{\varepsilon}) \mathbf{I} + 2\mu_s \boldsymbol{\varepsilon}$$

$$\text{with } \boldsymbol{\varepsilon} = \frac{1}{2} \{ (\bar{\nabla} \bar{u}) + (\bar{\nabla} \bar{u})^c \}, \text{tr}(\boldsymbol{\varepsilon}) = \bar{\nabla} \cdot \bar{u}$$

$$\sigma^f = -p n^f \mathbf{I} - \frac{2}{3} \eta_a \text{tr}(D^f) \mathbf{I} + 2\eta_a D^f \quad (2.38)$$

$$\text{with } D^f = \frac{1}{2} \{ (\bar{\nabla} \bar{v}^f) + (\bar{\nabla} \bar{v}^f)^c \}, \text{tr}(D^f) = \bar{\nabla} \cdot \bar{v}^f$$

$$\bar{\pi}^s = \mathbf{K} (\bar{v}^f - \bar{v}^s)$$

$$\bar{\pi}^f = \mathbf{K} (\bar{v}^s - \bar{v}^f)$$

2.3.3. Equations of motion

The balance of mass is given by (2.23) :

$$\bar{\nabla} \cdot (\mathbf{n}^f(\bar{\mathbf{v}}^f - \bar{\mathbf{v}}^s)) + \bar{\nabla} \cdot \bar{\mathbf{v}}^s = 0 \quad (2.39)$$

Substituting the constitutive relations from (2.38) into the balance of momentum (2.23) yields:

$$\begin{aligned} \bar{\nabla} \cdot \boldsymbol{\sigma}^s + \bar{\pi}^s &= \\ -\bar{\nabla} (\mathbf{n}^s p) + \lambda_s \bar{\nabla} (\text{tr} \boldsymbol{\varepsilon}) + 2\mu_s (\bar{\nabla} \cdot \boldsymbol{\varepsilon}) + \mathbf{K}(\bar{\mathbf{v}}^f - \bar{\mathbf{v}}^s) &= \\ -\bar{\nabla} (\mathbf{n}^s p) + (\lambda_s + \mu_s) \bar{\nabla} (\bar{\nabla} \cdot \bar{\mathbf{u}}) + \mu_s \bar{\nabla} \cdot (\bar{\nabla} \bar{\mathbf{u}}) + \mathbf{K}(\bar{\mathbf{v}}^f - \bar{\mathbf{v}}^s) &= \bar{\boldsymbol{\sigma}} \end{aligned} \quad (2.40)$$

$$\begin{aligned} \bar{\nabla} \cdot \boldsymbol{\sigma}^f - \bar{\pi}^f &= \\ -\bar{\nabla} (\mathbf{n}^f p) - \eta_a \bar{\nabla} (\text{tr} \mathbf{D}^f) + 2\eta_a (\bar{\nabla} \cdot \mathbf{D}^f) - \mathbf{K}(\bar{\mathbf{v}}^f - \bar{\mathbf{v}}^s) &= \\ -\bar{\nabla} (\mathbf{n}^f p) + \frac{1}{3} \eta_a \bar{\nabla} (\bar{\nabla} \cdot \bar{\mathbf{v}}^f) + \eta_a \bar{\nabla} \cdot (\bar{\nabla} \bar{\mathbf{v}}^f) - \mathbf{K}(\bar{\mathbf{v}}^f - \bar{\mathbf{v}}^s) &= \bar{\boldsymbol{\sigma}} \end{aligned} \quad (2.41)$$

Using vector identities with respect to a cylindrical coordinate system (see Appendix I), the equations above can be expressed by :

(2.42):

$$\frac{1}{r} \frac{\partial n^f r (v_r^f - v_r^s)}{\partial r} + \frac{\partial n^f (v_z^f - v_z^s)}{\partial z} + \frac{1}{r} \frac{\partial r v_r^s}{\partial r} + \frac{\partial v_z^s}{\partial z} = 0$$

(2.43):

$$\begin{aligned} -n^s \frac{\partial p}{\partial r} + (\lambda_s + \mu_s) \frac{\partial}{\partial r} \left(\frac{u_r}{r} + \frac{\partial u_r}{\partial r} + \frac{\partial u_z}{\partial z} \right) + \mu_s \frac{\partial}{\partial r} \left(\frac{u_r}{r} + \frac{\partial u_r}{\partial r} \right) + \mu_s \frac{\partial^2 u_r}{\partial z^2} + \\ + K(v_r^f - v_r^s) = 0 \\ -n^s \frac{\partial p}{\partial z} + (\lambda_s + \mu_s) \frac{\partial}{\partial z} \left(\frac{u_r}{r} + \frac{\partial u_r}{\partial r} + \frac{\partial u_z}{\partial z} \right) + \mu_s \frac{1}{r} \frac{\partial}{\partial r} \left(r \frac{\partial u_z}{\partial r} \right) + \mu_s \frac{\partial^2 u_z}{\partial z^2} + \\ + K(v_z^f - v_z^s) = 0 \end{aligned}$$

(2.44):

$$\begin{aligned} -n^f \frac{\partial p}{\partial r} + \frac{1}{3} \eta_a \frac{\partial}{\partial r} \left(\frac{v_r^f}{r} + \frac{\partial v_r^f}{\partial r} + \frac{\partial v_z^f}{\partial z} \right) + \eta_a \frac{\partial}{\partial r} \left(\frac{v_r^f}{r} + \frac{\partial v_r^f}{\partial r} \right) + \eta_a \frac{\partial^2 v_r^f}{\partial z^2} + \\ - K(v_r^f - v_r^s) = 0 \\ -n^f \frac{\partial p}{\partial z} + \frac{1}{3} \eta_a \frac{\partial}{\partial z} \left(\frac{v_r^f}{r} + \frac{\partial v_r^f}{\partial r} + \frac{\partial v_z^f}{\partial z} \right) + \eta_a \frac{1}{r} \frac{\partial}{\partial r} \left(r \frac{\partial v_z^f}{\partial r} \right) + \eta_a \frac{\partial^2 v_z^f}{\partial z^2} + \\ - K(v_z^f - v_z^s) = 0 \end{aligned}$$

Cylinder-symmetry has been taken into account.

2.4. Boundary conditions

2.4.1. The indenter - fluid film interface

Through the indenter, a load $F(t)$ is exerted on the fluid. Neglecting inertia forces, the indenter load will be in equilibrium with the fluid normal stress in the z-direction σ_{zz}^f :

$$\int_0^{\infty} \int_0^{2\pi} \sigma_{zz}^f r d\varphi dr = -F(t) \quad (2.45)$$

In a first order approximation σ_{zz}^f is assumed to be equal to the hydrodynamic pressure $-p$. As a result of the indenter load, the indenter moves in the negative z-direction with a velocity $V(t)$. Assuming a no-slip kinematic boundary condition at the indenter - fluid film interface, it holds :

$$\vec{v}^f (r, z=g(r,t), t) = -V(t) \vec{e}_z \quad (2.46)$$

2.4.2. The fluid film - mixture interface

Hou (1989) considered the interface to be a 'surface of discontinuity', which is a material surface fixed to the solid phase. This choice is consistent with the idea that the geometrical boundary of a biphasic material is defined by the solid phase. Across the 'surface of discontinuity' any of the material properties of anyone of the phases may be discontinuous.

Kinematic boundary conditions at a surface of discontinuity within a biphasic material must reduce, in the limiting case of $n^f=0$ on one side of the surface and $n^s=0$ on the other side, to the regular no-slip condition. Hou (1989) formulated a *pseude-no-slip* condition satisfying the above principle :

The tangential component (parallel to the interface) of the volumefraction weighted average velocity of the mixture components has to be continuous across the surface of discontinuity.

where the following assumption is used:

assumption 14 The surface fractions are assumed to be equal to the volumefractions.

From application of the balance of mass for a volume element which is split into two parts by a surface of discontinuity, it can be concluded that a similar condition holds for the velocity component normal to the surface. The following *kinematic* boundary condition results :

$$n^s \bar{v}_-^s + n^f \bar{v}_-^f = \bar{v}_+^f \quad (2.47)$$

where the index + is reserved for the fluid film side of the interface, and the index – for the mixture side.

Elaboration of the balances of momentum and energy for a volume element which is split into two parts by a surface of discontinuity, using the pseudo-no-slip condition yields the following *dynamic* boundary conditions (Hou, 1989) :

$$\bar{n} \cdot \sigma_-^s = n^s \bar{n} \cdot \sigma_+^f \quad (2.48)$$

$$\bar{n} \cdot \sigma_-^f = n^f \bar{n} \cdot \sigma_+^f \quad (2.49)$$

These boundary conditions are known as jump conditions.

From the equations (2.48) and (2.49) it can be seen that the stress which is exerted on the mixture by the fluid, is distributed over the fluid and solid component of the mixture in accordance with the volume fractions n^f and n^s respectively.

If the unit outward normal of the mixture \bar{n} is equal to \bar{e}_z (see figure 3), the kinematic boundary condition (2.47) can be expressed in coordinates by :

$$(n^s v_r^s + n^f v_r^f)_{z=(g-h)^-} = (v_r^f)_{z=(g-h)^+} \quad (2.50)$$

$$(n^s v_z^s + n^f v_z^f)_{z=(g-h)^-} = (v_z^f)_{z=(g-h)^+} \quad (2.51)$$

and the dynamic boundary conditions (2.48) and (2.49) can be expressed in coordinates by :

z - direction :

$$\left(\lambda_s \frac{1}{r} \frac{\partial(ru_r)}{\partial r} + (\lambda_s + 2\mu_s) \frac{\partial u_z}{\partial z} \right)_{z=(g-h)^-} = 2n^s \eta_f \left(\frac{\partial v_z^f}{\partial z} \right)_{z=(g-h)^+} \quad (2.52)$$

r - direction :

$$\mu_s \left(\frac{\partial u_r}{\partial z} + \frac{\partial u_z}{\partial r} \right)_{z=(g-h)^-} = n^s \eta_f \left(\frac{\partial v_r^f}{\partial z} + \frac{\partial v_z^f}{\partial r} \right)_{z=(g-h)^+} \quad (2.53)$$

z - direction :

$$\eta_a \left(-\frac{1}{3} \frac{1}{r} \frac{\partial(rv_r)}{\partial r} + \frac{2}{3} \frac{\partial v_z}{\partial z} \right)_{z=(g-h)^-} = n^f \eta_f \left(\frac{\partial v_z}{\partial z} \right)_{z=(g-h)^+} \quad (2.54)$$

r - direction :

$$\eta_a \left(\frac{\partial v_r}{\partial z} + \frac{\partial v_z}{\partial r} \right)_{z=(g-h)^-} = n^f \eta_f \left(\frac{\partial v_r}{\partial z} + \frac{\partial v_z}{\partial r} \right)_{z=(g-h)^+} \quad (2.55)$$

2.4.3. The mixture - subchondral bone interface

At the interface between the cartilage and the rigid subchondral bone ($z=0$), no-slip boundary conditions are assumed :

$$\vec{u}(r, z=0, t) = \vec{0} \quad (2.56)$$

$$\vec{v}^f(r, z=0, t) = \vec{0} \quad (2.57)$$

2.4.4. Additional boundary conditions

Finally, the solution has to satisfy the ambient conditions for the pressure and displacement :

$$p(r, z, t) \rightarrow 0 \text{ voor } r \rightarrow \infty \quad (2.58)$$

$$\vec{u}(r, z, t) \rightarrow \vec{0} \text{ voor } r \rightarrow \infty \quad (2.59)$$

$$\vec{v}^f(r, z, t) \rightarrow \vec{0} \text{ voor } r \rightarrow \infty \quad (2.60)$$

If the load carrying area has a radius R_0 , with $R_0 < R_p$, the pressure p and the solid displacement \vec{u} are supposed to be 0 for $r > R_0$.

2.5. Summary of equations and boundary conditions

In the last section of this chapter, a summary will be given of the basic equations and the obtained boundary conditions.

Fluid film:

- ▶ balance of mass:

$$\vec{\nabla} \cdot \vec{v}^f = 0 \quad (2.61)$$

- ▶ balance of momentum:

$$-\vec{\nabla} p + \eta_f \vec{\nabla} \cdot (\vec{\nabla} \vec{v}^f) = \vec{\sigma} \quad (2.62)$$

- ▶ unknown variables: p, \vec{v}^f .

Cartilage layer:

- ▶ balance of mass:

$$\vec{\nabla} \cdot (\mathbf{n}^f (\vec{v}^f - \vec{v}^s)) + \vec{\nabla} \cdot \vec{v}^s = 0 \quad (2.63)$$

- ▶ balance of momentum:

$$-\vec{\nabla} (\mathbf{n}^s p) + (\lambda_s + \mu_s) \vec{\nabla} (\vec{\nabla} \cdot \vec{u}) + \mu_s \vec{\nabla} \cdot (\vec{\nabla} \vec{u}) + K(\vec{v}^f - \vec{v}^s) = \vec{\sigma} \quad (2.64)$$

$$-\vec{\nabla} (\mathbf{n}^f p) + \frac{1}{3} \eta_a \vec{\nabla} (\vec{\nabla} \cdot \vec{v}^f) + \eta_a \vec{\nabla} \cdot (\vec{\nabla} \vec{v}^f) - K(\vec{v}^f - \vec{v}^s) = \vec{\sigma} \quad (2.65)$$

- ▶ moreover:

$$\frac{\partial \vec{u}}{\partial t} = \vec{v}^s \quad (2.66)$$

- ▶ unknown variables: $p, \vec{v}^f, \vec{v}^s, \vec{u}$.

As well for the fluid film as for the cartilage layer there are as many equations as unknown variables, so it may be possible to solve this problem, if sufficient boundary conditions are available.

Boundary conditions:

Since the highest order of the three leading differential equations (2.62), (2.64) and (2.65) is equal to 2, it is possible to solve the problem if 6 boundary conditions can be formulated :

- ▶ at the surface of the spherical indenter ($z = g(r,t)$):

$$\vec{v}^f = V(t) \vec{e}_z \quad (2.67)$$

- ▶ at the interface between the fluid film and the cartilage layer ($z = H_0$):

$$\vec{e}_z \cdot \{ \lambda_s \text{tr}(\boldsymbol{\varepsilon}) \mathbf{I} + 2\mu_s \boldsymbol{\varepsilon} \} = n^s \vec{e}_z \cdot \{ 2\eta_f \mathbf{D}^f \} \quad (2.68)$$

$$\vec{e}_z \cdot \{ -\frac{2}{3}\eta_a \text{tr}(\mathbf{D}^f) \mathbf{I} + 2\eta_a \mathbf{D}^f \} = n^f \vec{e}_z \cdot \{ 2\eta_f \mathbf{D}^f \} \quad (2.69)$$

$$n^s \vec{v}_-^s + n^f \vec{v}_-^f = \vec{v}_+^f \quad (2.70)$$

- ▶ at the surface of the subchondral bone ($z = 0$):

$$\vec{u} = \vec{0} \quad (2.71)$$

$$\vec{v}^f = \vec{0} \quad (2.72)$$

In the equations above $\boldsymbol{\varepsilon}$ is the linear deformation tensor of the solid and \mathbf{D}^f is the rate of deformation tensor of the fluid.

Chapter 3. Solution of the equations of motion for three special cases

3.1. Introduction

Having the equations of motion (§ 2.2, 2.3) and the boundary conditions (§ 2.4), it should be possible to calculate the pressure distribution over the model, the deformation of the cartilage layers and the fluid flow throughout the model, which results from application of a load on the indenter. Hou (1989) performs these calculations almost fully analytically, but he is therefore restricted to a stepload on the indenter. At first instance, in this study, no restrictions are imposed upon the load.

Three special cases of Hou's squeeze film model will be investigated, i.e.:

- two rigid impermeable approaching circular plates (section 3.2),
- a rigid impermeable spherical indenter approaching a rigid impermeable plane (section 3.3),
- a rigid impermeable circular plate approaching a rigid permeable biphasic fluid-solid mixture (section 3.4).

For each case a system of equations is derived, which will be used to determine numerically the film thickness as a function of time. Although an arbitrary load may be applied, in this report a stepload is used to facilitate comparison of the results for the successive cases.

3.2. Two rigid impermeable parallel approaching plates

3.2.1. Problem definition

Within the gap between two rigid impermeable circular plates with radius R_0 a Newtonian fluid with viscosity η_f is found (figure 4). The distance between the plates $h(t)$ is, unlike the figure suggests, much smaller than the radius of the plates R_0 .

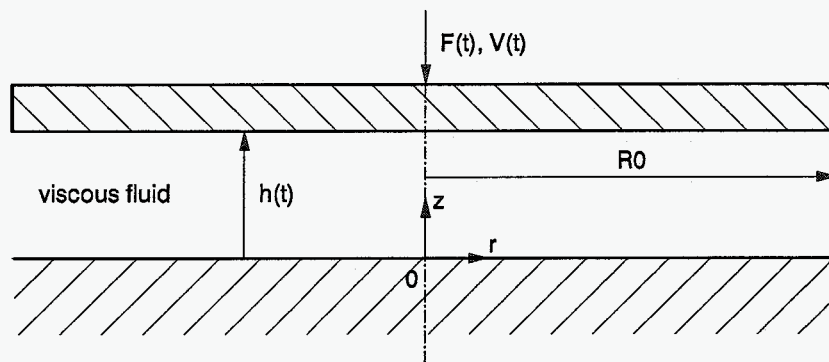


figure 4 A squeeze film between two rigid impermeable parallel approaching plates

A prescribed load $F(t)$ is applied to the upper plate in the negative z -direction. As a result of $F(t)$, the plate starts moving into the negative z -direction with a velocity $V(t)$. The position of the surface of the upper plate is represented by the function $h(t)$:

$$h(t) = h(t=0) - \int_0^t V(\tau) d\tau = h_0 - \int_0^t V(\tau) d\tau \quad (3.1)$$

At the surfaces of the plates the no-slip condition is valid, resulting in the following boundary conditions:

$$\begin{aligned} z = h(t) : v_r &= 0, v_z = -V(t) \\ z = 0 : v_r &= 0, v_z = 0 \end{aligned} \quad (3.2)$$

The scaling factor for the squeeze film thickness is chosen to be h_0 , the initial film thickness. The ratio of h_0 and R_0 yields an important geometrical variable α , which will be used to expand the variables into power series :

$$\alpha = \frac{h_0}{R_0} \ll 1. \quad (3.3)$$

3.2.2. Simplification of the equations of motion using power series expansions

To get a general and simplified formulation of the equations of motion the variables are scaled according to:

$$r' = \frac{r}{R_0}, \quad z' = \frac{z}{h_0}, \quad h' = \frac{h}{h_0}, \quad t' = \frac{t}{t_0} \quad (3.4)$$

$$v'_r = \frac{v_r}{V_0}, \quad v'_z = \frac{v_z}{V_0}, \quad V'(t) = \frac{V(t)}{V_0}$$

$$F'(t) = \frac{F(t)}{F_0}, \quad p' = \frac{p}{P_0}$$

where V_0 is a characteristic value of the velocity of the upper plate,

F_0 is a characteristic value of the load on the upper plate,

$$P_0 = F_0 / (\pi R_0^2),$$

t_0 is the time scaling factor.

After scaling the balance of mass for the fluid film (2.9) becomes:

$$\frac{\partial v'_z}{\partial z'} = -\alpha \frac{1}{r'} \frac{\partial(r' v'_r)}{\partial r'} \quad (3.5)$$

v_z' appears to be of the same order as $\alpha v_r'$. Since $\alpha \ll 1$, v_r' is of much higher order than v_z' . In order to obtain a simple system of differential equations, v_r will be rescaled :

$$v_r'' = \alpha \frac{v_r}{V_0} \quad (3.6)$$

After rescaling the balance of mass becomes (accents are left out) :

$$\frac{\partial v_z}{\partial z} = -\frac{1}{r} \frac{\partial(r v_r)}{\partial r} \quad (3.7)$$

The balance of momentum (2.10) becomes :

$$-\frac{P_0 h_0^3}{\eta_f V_0 R_0^2} \frac{\partial p}{\partial r} + \alpha^2 \frac{\partial}{\partial r} \left(\frac{\partial v_r}{\partial r} + \frac{v_r}{r} \right) + \frac{\partial^2 v_r}{\partial z^2} = 0 \quad (3.8)$$

$$-\frac{P_0 h_0^3}{\eta_f V_0 R_0^2} \frac{\partial p}{\partial z} + \alpha^4 \frac{1}{r} \frac{\partial}{\partial r} \left(r \frac{\partial v_z}{\partial r} \right) + \alpha^2 \frac{\partial^2 v_z}{\partial z^2} = 0 \quad (3.9)$$

The scaling factor V_0 is chosen in such a way that :

$$\frac{P_0 h_0^3}{\eta_f V_0 R_0^2} = 1 \quad (3.10)$$

Substituting the relation for P_0 in (3.10) yields :

$$V_0 = \frac{F_0 h_0^3}{\pi \eta_f R_0^4} \quad (3.11)$$

This choice for V_0 prevents important zero order terms from disappearing out of the momentum equations when power series are substituted.

Next, the dependent variables are expanded in terms of powers of α :

$$p(r, z, t) = p^{(0)}(r, z, t) + p^{(1)}(r, z, t)\alpha + p^{(2)}(r, z, t)\alpha^2 + \dots, \quad (3.12)$$

$$v_r(r, z, t) = v_r^{(0)}(r, z, t) + v_r^{(1)}(r, z, t)\alpha + v_r^{(2)}(r, z, t)\alpha^2 + \dots, \quad (3.13)$$

$$v_z(r, z, t) = v_z^{(0)}(r, z, t) + v_z^{(1)}(r, z, t)\alpha + v_z^{(2)}(r, z, t)\alpha^2 + \dots, \quad (3.14)$$

Substituting these power series into the equations of motion and collecting terms of equal power in α yields the following differential equations in the coefficients of the power series:

balance of mass (3.7):

$$\frac{\partial v_z^{(0)}}{\partial z} = -\frac{1}{r} \frac{\partial(r v_r^{(0)})}{\partial r} \quad (3.15)$$

$$\frac{\partial v_z^{(1)}}{\partial z} = -\frac{1}{r} \frac{\partial(r v_r^{(1)})}{\partial r} \quad (3.16)$$

$$\frac{\partial v_z^{(2)}}{\partial z} = -\frac{1}{r} \frac{\partial(r v_r^{(2)})}{\partial r} \quad (3.17)$$

balance of momentum in r-direction (3.8):

$$\frac{\partial p^{(0)}}{\partial r} = \frac{\partial^2 v_r^{(0)}}{\partial z^2} \quad (3.18)$$

$$\frac{\partial p^{(1)}}{\partial r} = \frac{\partial^2 v_r^{(1)}}{\partial z^2} \quad (3.19)$$

$$\frac{\partial p^{(2)}}{\partial r} = \frac{\partial}{\partial r} \left(\frac{\partial v_r^{(0)}}{\partial r} + \frac{v_r^{(0)}}{r} \right) + \frac{\partial^2 v_r^{(2)}}{\partial z^2} \quad (3.20)$$

balance of momentum in z-direction (3.9):

$$\frac{\partial p^{(0)}}{\partial z} = 0 \quad (3.21)$$

$$\frac{\partial p^{(1)}}{\partial z} = 0 \quad (3.22)$$

$$\frac{\partial p^{(2)}}{\partial z} = \frac{\partial^2 v_z^{(0)}}{\partial z^2} \quad (3.23)$$

Finally the boundary conditions are scaled and rewritten as conditions on to the coefficients of the power series :

$z = h(t)$:

$$v_r = 0 \quad \Rightarrow \quad v_r^{(0)} = 0 \quad , \quad v_r^{(1)} = 0 \quad , \quad v_r^{(2)} = 0 \quad (3.24)$$

$$v_z = -V(t) \quad \Rightarrow \quad v_z^{(0)} = -V(t) \quad , \quad v_z^{(1)} = 0 \quad , \quad v_z^{(2)} = 0 \quad (3.25)$$

$z = 0$:

$$v_r = 0 \quad \Rightarrow \quad v_r^{(0)} = 0 \quad , \quad v_r^{(1)} = 0 \quad , \quad v_r^{(2)} = 0 \quad (3.26)$$

$$v_z = 0 \quad \Rightarrow \quad v_z^{(0)} = 0 \quad , \quad v_z^{(1)} = 0 \quad , \quad v_z^{(2)} = 0 \quad (3.27)$$

A first order approximation is found by neglecting higher order terms of the power series (order α^2 and higher), which is permitted since $\alpha \ll 1$.

3.2.3. Film thickness and pressure distribution over the squeeze film

Solving the differential equations, given the boundary conditions above, yields :

$$v_r^{(0)}(r, z, t) = \frac{1}{2} \frac{\partial p^{(0)}}{\partial r} (z^2 - h(t) z) \quad (3.28)$$

$$v_r^{(1)}(r, z, t) = 0$$

$$v_z^{(0)}(r, z, t) = -\frac{1}{2} \frac{1}{r} \frac{\partial}{\partial r} \left(r \left(\frac{1}{3} z^3 - \frac{1}{2} h(t) z^2 \right) \frac{\partial p^{(0)}}{\partial r} \right) \quad (3.29)$$

$$v_z^{(1)}(r, z, t) = 0$$

$$p^{(0)}(r, z, t) = p^{(0)}(r, t) \quad (3.30)$$

$$p^{(1)}(r, z, t) = 0$$

A first order approximation is thus :

$$v_r(r, z, t) = \frac{1}{2} \frac{\partial p}{\partial r} (z^2 - h(t) z) \quad (3.31)$$

$$v_z(r, z, t) = -\frac{1}{2} \frac{1}{r} \frac{\partial}{\partial r} \left(r \left(\frac{1}{3} z^3 - \frac{1}{2} h(t) z^2 \right) \frac{\partial p}{\partial r} \right) \quad (3.32)$$

$$p(r, z, t) = p(r, t) \quad (3.33)$$

Since both the pressure and the pressure gradient are independent of the z-coordinate, the radial fluid velocity v_r forms a parabolic velocity profile, as expected. The relation between the upper plate velocity, the film thickness and the pressure gradient is found by substituting boundary condition (3.25) into equation (3.32), which results in a special case of the Reynolds-equation, an equation which is often used in tribology :

$$V(t) = -\frac{1}{12 r} \frac{\partial}{\partial r} \left(r h^3(t) \frac{\partial p}{\partial r} \right) \quad (3.34)$$

Since the film thickness for a squeeze film between two parallel rigid plates is no function of the r -coordinate, the Reynolds-equation (3.34) can be rewritten as :

$$V(t) = -\frac{h^3(t)}{12} \frac{1}{r} \frac{\partial}{\partial r} \left(r \frac{\partial p}{\partial r} \right) \quad (3.35)$$

Integration of this equation from 0 to r and subsequently from r to 1, given two pressure boundary conditions :

$$r = 1 : \quad p(r,t) = 0 \quad (3.36)$$

$$r = 0 : \quad \frac{\partial p}{\partial r} = 0 , \quad (3.37)$$

yields :

$$p(r,t) = \frac{3 V(t)}{h^3(t)} (1 - r^2) \quad (3.38)$$

This relation was derived by Michell in 1950 (Michell, 1950).

In order to solve this squeeze film problem however, two more equations are required, i.e. a relation between the film thickness $h(t)$ and the upper plate velocity $V(t)$ (3.1) and a relation between the load on the upper plate $F(t)$ and the pressure distribution $p(r,t)$ ((2.45), § 2.4):

$$h(t) = h_0 - \int_0^t V(\tau) d\tau \quad (3.39)$$

$$2\pi \int_0^{R_0} p(r,t) r dr = F(t) \quad (3.40)$$

Scaling these equations yields :

$$h(t) = 1 - \frac{V_0 t_0}{h_0} \int_0^t V(\tau) d\tau \quad (3.41)$$

$$2 \int_0^1 p(r,t) r dr = F(t) \quad (3.42)$$

The scaling factor for the time t_0 may be chosen arbitrarily. If t_0 is chosen to be:

$$t_0 = \frac{h_0}{V_0} \quad (3.43)$$

the following system of equations results :

$$\begin{aligned} p(r,t) &= \frac{3 V(t)}{h^3(t)} (1 - r^2) \\ h(t) &= 1 - \int_0^t V(\tau) d\tau \\ F(t) &= 2 \int_0^1 p(r,t) r dr \end{aligned} \quad (3.44)$$

The load on the upper plate $F(t)$ will be prescribed.

Since the film thickness $h(t)$ is no function of the r -coordinate these equations may be rewritten as:

$$F(t) = \frac{3}{2} \frac{V(t)}{h^3(t)} \quad \text{with:} \quad h(t) = \left(1 - \int_0^t V(\tau) d\tau \right) \quad (3.45)$$

$$p(r,t) = 2 F(t) (1 - r^2) \quad \text{for} \quad r \leq 1 \quad (3.46)$$

To obtain these resulting equations, the pressure is integrated over the load carrying area. This solution is in accordance with literature (O'Connor and Boyd, 1968).

When the load on the upper plate is given as a function of time, the nonlinear equation (3.45) can be solved iteratively with the algorithm given in appendix II.2.1. Although the load may be an arbitrary function of time, a stepload ($F(t)=0$ for $t<0$ and $F(t)=1$ for $t\geq 0$) is applied to the upper plate in order to facilitate interpretation and comparison of the results. In figure 5 the pressure distribution over the fluid film is shown :

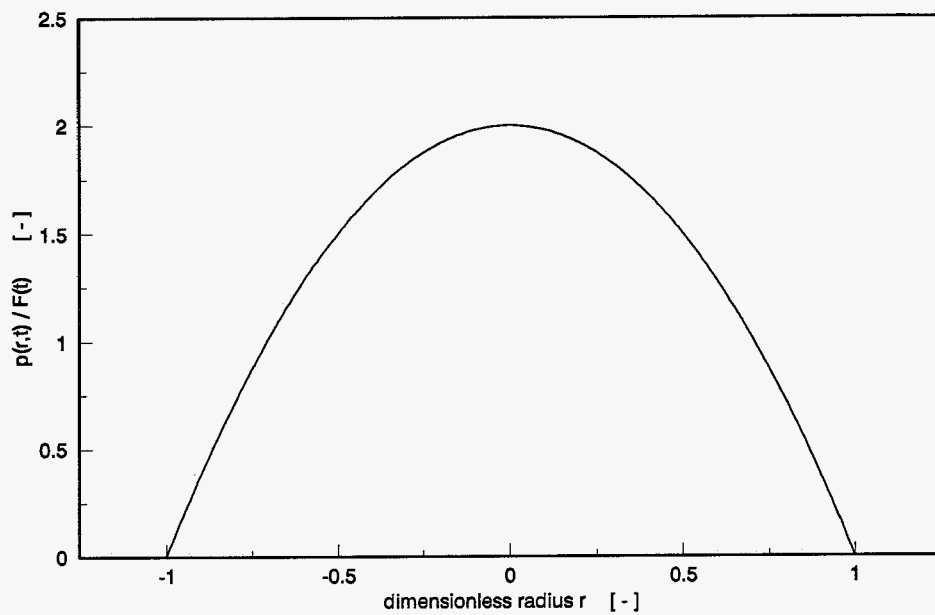


figure 5 The dimensionless pressure distribution (divided by the dimensionless load $F(t)$) over the squeeze film

figure 6 shows the calculated film thickness $h(t)$ versus time. As a result of the load, the fluid is forced out from between the two plates, while the gap between the plates gets smaller. The smaller the gap is however, the higher is the resistance for the fluid to flow out. Therefore the upper plate velocity decreases with time.

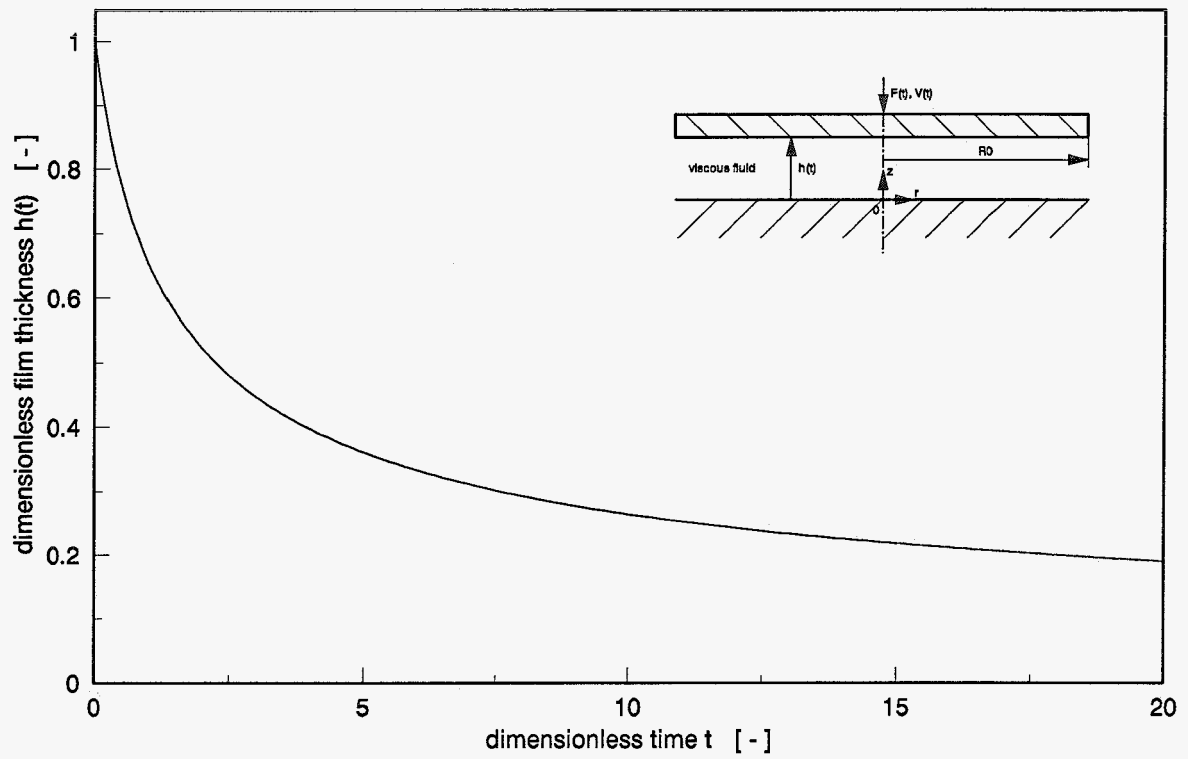


figure 6 *Dimensionless filmthickness $h(t)$ versus time, when a stepload is applied to the upper plate at $t=0$.*

In the next section the fluid film between a spherical indenter and a rigid plane will be investigated.

3.3. A rigid impermeable spherical indenter approaching a rigid impermeable plane

3.3.1. Problem definition

Between a rigid impermeable spherical indenter with radius R_i and a rigid impermeable plane, a Newtonian fluid with viscosity η_f (figure 7) is found. The minimal distance between the indenter and the plane $h(0,t)$ is, unlike the figure suggests, much smaller than R_0 , the radius of the load transmitting area.

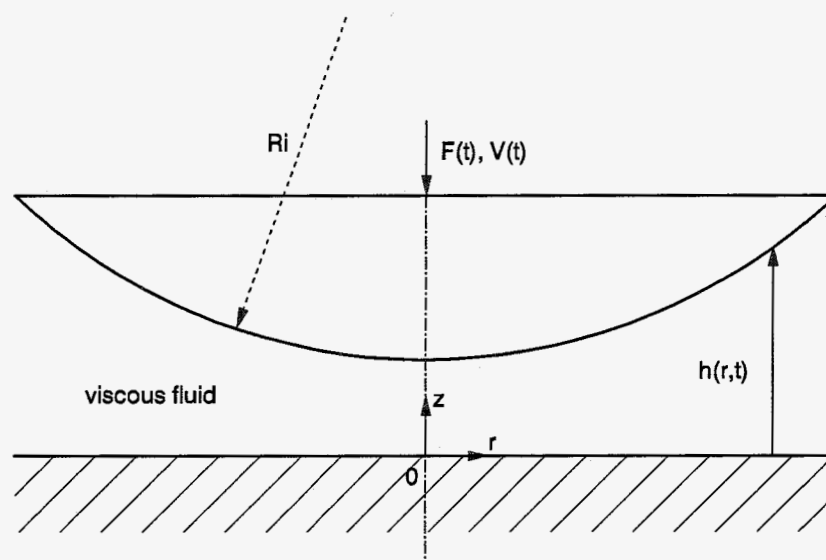


figure 7 *A squeeze film between a rigid impermeable spherical indenter and a rigid impermeable plane*

A prescribed load $F(t)$ is applied to the indenter in the negative z -direction. As a result of $F(t)$, the indenter starts moving into the negative z -direction with velocity $V(t)$. The position of the surface of the indenter is represented by the function $h(r,t)$:

$$h(r,t) = h(r,0) - \int_0^t V(\tau) d\tau \quad (3.47)$$

At the surfaces of the indenter and the plate, the no-slip condition is valid, resulting in the following boundary conditions:

$$\begin{aligned} z = h(r,t) : v_r &= 0, v_z = -V(t) \\ z = 0 : v_r &= 0, v_z = 0 \end{aligned} \quad (3.48)$$

The scaling factor for the squeeze film thickness is chosen to be $h_0 = h(0,0)$, the initial minimal film thickness. The variables will be expanded into power series of α :

$$\alpha = \frac{h_0}{R_0} . \quad (3.49)$$

3.3.2. Film thickness and pressure distribution over the squeeze film

Scaling according to (3.4) and rewriting the equations of motion (§ 3.2.2) results in the Reynolds-equation :

$$V(t) = - \frac{1}{12 r} \frac{\partial}{\partial r} \left(r h^3(r,t) \frac{\partial p}{\partial r} \right) \quad (3.50)$$

Integration of this equation from 0 to r with :

$$r = 0 : \frac{\partial p}{\partial r} = 0 , \quad (3.51)$$

yields :

$$\frac{\partial p}{\partial r} = \frac{-6 V(t) r}{h^3(r,t)} \quad (3.52)$$

The pressure distribution $p(r,t)$ is obtained by integrating (3.52) from r to ∞ with the formal boundary condition $p(r \rightarrow \infty, t) = 0$. By evaluation of the pressure distribution $p(r,t)$, the pressure appears to approximate to 0 at a finite distance from the axis of symmetry $R_0 < R_i$:

$$r \geq 1 : p(r,t) = 0 . \quad (3.53)$$

The scaling factor R_0 is not previously known. To determine R_0 , the pressure distribution will be calculated for increasing values of R_0 at $t = 0^+$. Above a certain value of R_0 , the pressure distributions do apparently not differ from each other. This specific value of R_0 will be chosen to be the scaling factor for the radius.

In order to integrate (3.52) a relation for the film thickness $h(r,t)$ in r and t is required. This relation only depends on the geometry of the indenter.

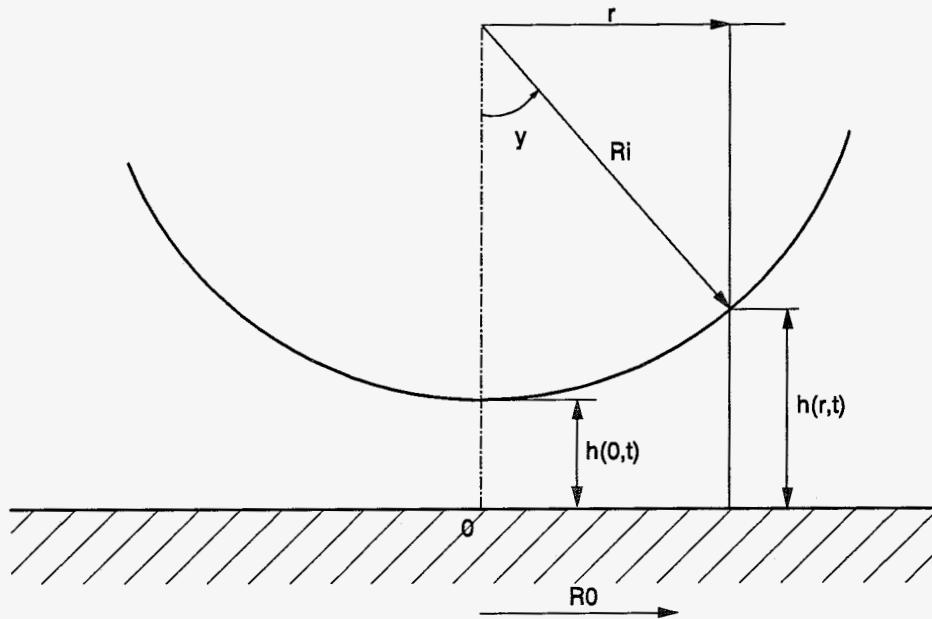


figure 8 The film thickness $h(r,t)$

The coordinates of the centre of the sphere are : $(0, h(0,t) + R_i)$.

The surface of the sphere is described by the following equation :

$$\{ (R_i + h(0,t)) - h(r,t) \}^2 + r^2 = R_i^2, \quad -R_0 < r < R_0 \quad (3.54)$$

The minimal distance between sphere and plane $h(0,t)$ depends on the time t according to :

$$h(0,t) = h(0,0) - \int_0^t V(\tau) d\tau = h_0 - \int_0^t V(\tau) d\tau \quad (3.55)$$

Rewriting (3.54) and using dimensionless variables yields :

$$h(r,t) = H(t) - \frac{1}{h_0} \sqrt{R_i^2 - (R_0 r)^2} \quad , \quad -1 < r < 1 \quad (3.56)$$

with :

$$H(t) = \frac{1}{h_0} (R_i + h_0) - \int_0^t V(\tau) d\tau \quad (3.57)$$

Substitution of the relation for $h(r,t)$ into (3.52) , and integration of the result from r to 1 with boundary condition (3.53) yields the pressure distribution as function of r and t :

$$p(r,t) = \quad (3.58)$$

$$3 \alpha^2 V(t) \left\{ H(t) \left(\frac{1}{h^2(r,t)} - \frac{1}{h^2(1,t)} \right) - 2 \left(\frac{1}{h(r,t)} - \frac{1}{h(1,t)} \right) \right\}$$

for $r \leq 1$.

In summary, the equations which have to be solved are given by :

$$p(r,t) =$$

$$3 \alpha^2 V(t) \left\{ H(t) \left(\frac{1}{h^2(r,t)} - \frac{1}{h^2(1,t)} \right) - 2 \left(\frac{1}{h(r,t)} - \frac{1}{h(1,t)} \right) \right\}$$

for $r \leq 1$,

$$h(r,t) = H(t) - \frac{1}{h_0} \sqrt{R_i^2 - (R_0 r)^2}$$

$$H(t) = \frac{1}{h_0} (R_i + h_0) - \int_0^t V(\tau) d\tau$$

$$F(t) = 2 \int_0^1 p(r,t) r dr \quad (3.59)$$

It is not easy to obtain (analytically nor numerically) the minimal film thickness $h(0,t)$ as a function of time from the system of equations given by (3.59). Since appreciable lubricating pressure is developed only in the region of small angles γ (figure 8), it is very common in tribology to approximate the film thickness in this region by a polynomial in r (Gross e.a., 1980) :

$$h(r,t) = h(0,t) + \frac{1}{2} \frac{r^2}{R_i} \quad (3.60)$$

The real film thickness (3.54) and the approximated film thickness (3.60) for $t = 0^+$ and $R_i = 50$ mm are shown in figure 9 :

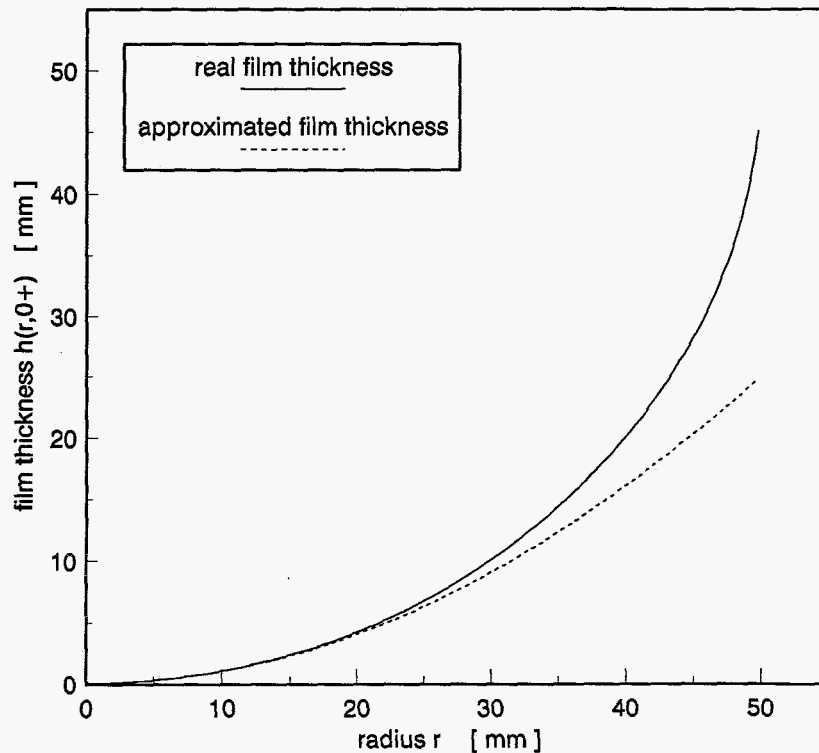


figure 9 The real and approximated film thickness as a function of r for $t = 0^+$, and $R_i = 50$ mm.

Using dimensionless variables, (3.60) becomes :

$$h(r,t) = h(0,t) + \frac{1}{2} \frac{R_0^2}{R_i h_0} r^2 = 1 - \int_0^t V(\tau) d\tau + \frac{1}{2} \frac{R_0^2}{R_i h_0} r^2 \quad (3.61)$$

Integrating (3.52) again from r to 1, using (3.61) yields :

$$p(r,t) = \frac{3 V(t) R_i h_0}{R_0^2} \left(\frac{1}{h^2(r,t)} - \frac{1}{h^2(1,t)} \right) \text{ for } r \leq 1 \quad (3.62)$$

which is a drastic simplification of the pressure distribution given by (3.58).

Integrating $p(r,t)$ over the load carrying area yields a relation between the indenter load $F(t)$, the indenter velocity $V(t)$ and the film thickness at $r = 0$ and $r = 1$:

$$F(t) = \frac{3}{2} \frac{V(t)}{h(0,t) h^2(1,t)}$$

with : $h(0,t) = 1 - \int_0^t V(\tau) d\tau$ (3.63)

and : $h(1,t) = h(0,t) + \frac{1}{2} \frac{R_0^2}{R_i h_0}$

Because the dimensionless film thickness $h(1,t)$ is an explicit function of the parameters h_0 , R_i , and R_0 , R_0 has to be determined given the values for R_i and h_0 . This has to be done in the dimensionfull space by calculating the pressure distribution at $t = 0^+$, when a stepload $F(t) = F_0$ for $t \geq 0$ is applied to the indenter :

$$p(r,0^+) = 3\eta_f R_i V(0^+) \left(\frac{1}{h^2(r,0^+)} - \frac{1}{h^2(R_0,0^+)} \right), \quad r \leq R_0 \quad (3.64)$$

where $V(0^+)$ is given by :

$$V(0^+) = \frac{2}{3} \frac{F_0}{\pi \eta_f R_0^4} h(0,0^+) h^2(R_0,0^+) \quad (3.65)$$

In figure 10 the pressure distribution $p(r,0^+)$ divided by F_0 is shown for three different values of R_0 ($R_0 = 10, 20$, and 30 mm). The parameters R_p , h_0 and η_f are chosen in accordance with Hou's squeeze film model for the knee-joint (Hou 1989), i.e.: $R_1 = 50$ mm, $h_0 = 0.1$ mm, and $\eta_f = 1.0$ Pa s.

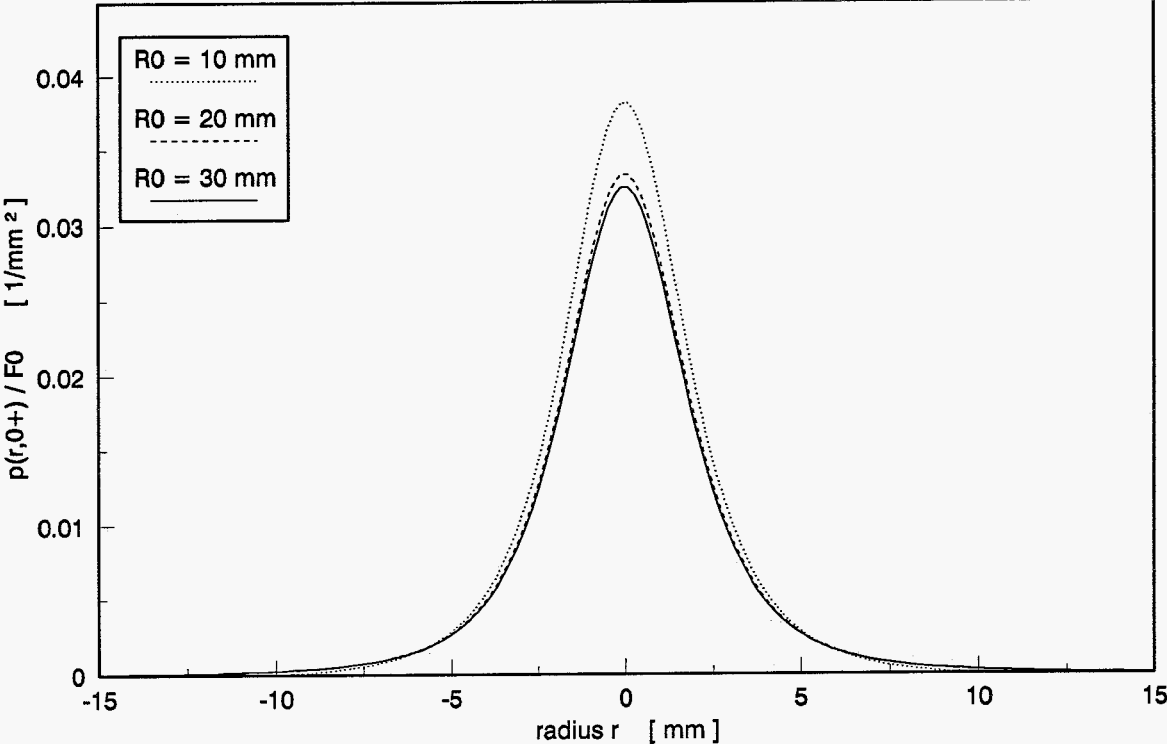


figure 10 The pressure distribution $p(r,0^+)$ divided by F_0 for three different values of the scaling factor R_0 (10, 20, and 30 mm) at $t = 0^+$

A marginal error between the two curves for $R_0 = 10$ mm and 20 mm can be seen, but the curves for $R_0 = 20$ mm and 30 mm are almost the same. Therefore R_0 is chosen to be 20 mm. For a radius $r \leq R_0 = 20$ mm, the approximated film thickness deviates from the real film thickness with less than 4 percent.

A stepload is applied to the spherical indenter at $t=0$ ($F(t)=0$ for $t<0$ and $F(t)=1$ for $t\geq 0$). The minimal film thickness versus time is calculated by solving the nonlinear equation (3.63) with the algorithm from appendix II.2.2. figure 11 shows the minimal film thickness $h(0,t)$ versus time:

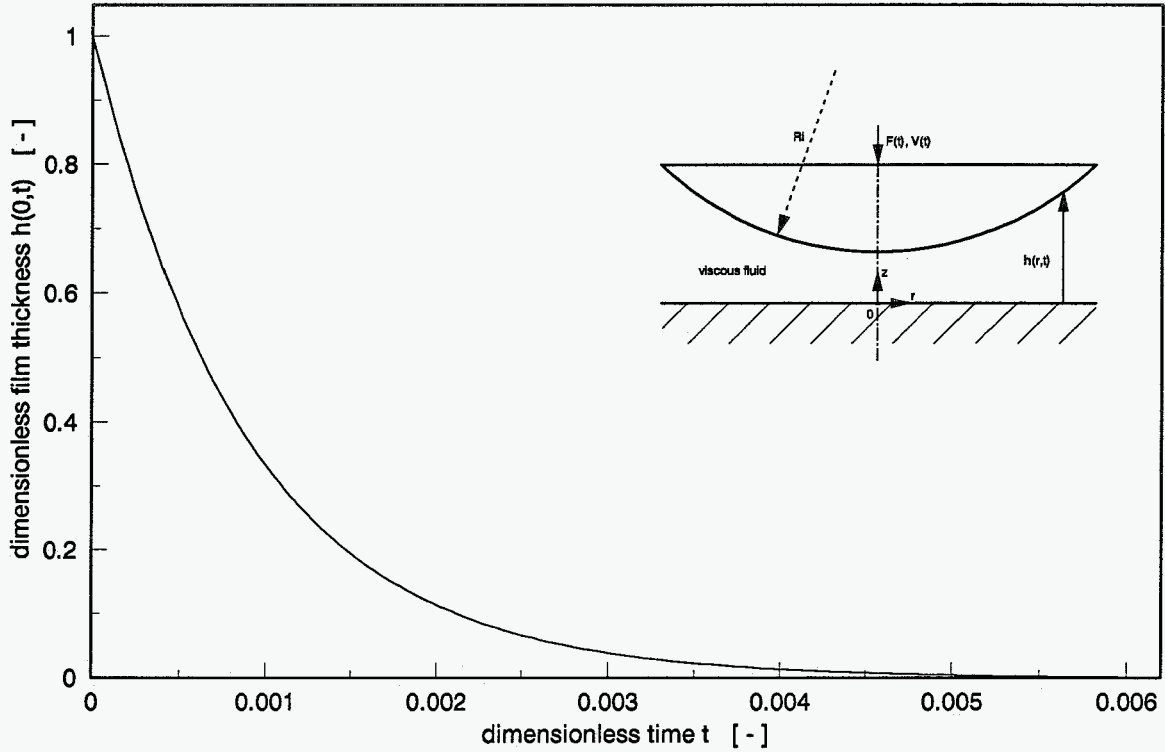


figure 11 Dimensionless minimal film thickness $h(0,t)$ versus time when a stepload is applied to the spherical indenter at $t=0$. ($R_i=50$ mm, $R_0=20$ mm, $h_0=0.1$ mm)

If compared with the solution for the first case (squeeze film between two plates) the film thickness decreases very fast. The fluid can easily flow out from between the spherical indenter and the plane, due to the geometry of the gap, which hardly changes with time.

It is remarkable however, that resembling equations have to be solved for the plate-plate and the sphere-plane configuration (compare equation (3.45) with (3.63)). These equations only differ because $h(1,t)$ is not equal to $h(0,t)$ when the film thickness depends on the radius r .

3.4. A rigid impermeable circular plate approaching a rigid permeable biphasic fluid-solid mixture

3.4.1. Problem definition

Within the gap between a rigid impermeable circular plate with radius R_0 and a rigid permeable biphasic fluid-solid mixture with porosity n^f and dragcoefficient K , a Newtonian fluid with viscosity η_f is found (figure 12). The viscosity of the interstitial fluid (fluid in the mixture) is equal to η_a (§ 2.3.2). The distance between the plate and the mixture $h(t)$ is, unlike the figure suggests much smaller than the radius of the plate R_0 .

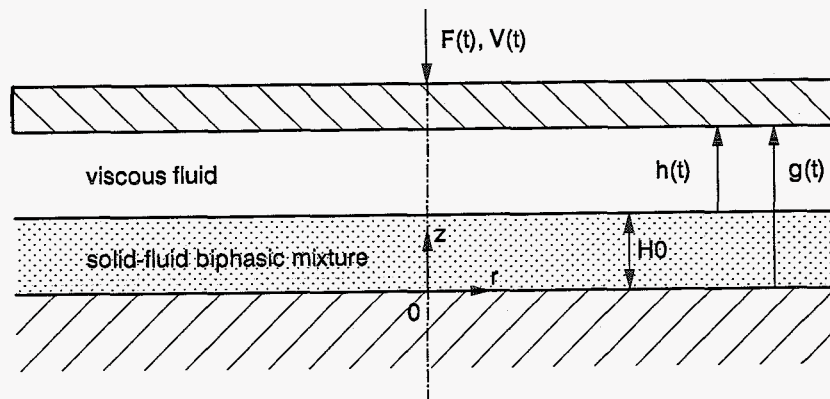


figure 12 A squeeze film between a rigid impermeable plate and a rigid permeable biphasic fluid-solid mixture

A prescribed load $F(t)$ is applied to the upper plate in the negative z -direction. As a result of $F(t)$, this plate starts moving into the negative z -direction with velocity $V(t)$. The position of the surface of the upper plate is represented by the function $g(t)$:

$$g(t) = H_0 + h(t) = H_0 + h_0 - \int_0^t V(\tau) d\tau \quad (3.66)$$

The equations of motion are separately solved for the squeeze film and the biphasic mixture. After that, the solutions will be matched by means of the interface boundary conditions.

3.4.2. Equations of motion for the fluid film

In this section the equations of motion will be solved for the fluid film. The resulting equations for v_r and v_z and the Reynolds-equation however hold two unknown variables, i.e. v_{rh} and v_{zh} , the radial and axial fluid velocity at the fluid-mixture interface respectively. These unknowns are determined by matching the solution for the squeeze film to that for the biphasic mixture.

At the surface of the plate, the no-slip condition is valid :

$$\begin{aligned} v_r(r, z=g, t) &= 0 \\ v_z(r, z=g, t) &= -V(t) \end{aligned} \quad (3.67)$$

At the interface the fluid velocity in r and z-direction are assumed to be equal to :

$$\begin{aligned} v_r(r, z=g-h, t) &= v_{rh}(r, t) \\ v_z(r, z=g-h, t) &= v_{zh}(r, t) \end{aligned} \quad (3.68)$$

In section 3.2.2 scaling of equations and power series expansions have already been discussed. This resulted in differential equations in the coefficients of the substituted power series :

balance of mass (3.15) and (3.16)
balance of momentum (3.18), (3.19), (3.21) and (3.22).

After scaling, the boundary conditions (3.67) and (3.68) can be rewritten as conditions on to the coefficients of the power series :

$z = g :$

$$v_r = 0 \quad \Rightarrow \quad v_r^{(0)} = 0 \quad , \quad v_r^{(1)} = 0 \quad (3.69)$$

$$v_z = -V(t) \quad \Rightarrow \quad v_z^{(0)} = -V(t) \quad , \quad v_z^{(1)} = 0 \quad (3.70)$$

$z = g - h :$

$$v_r = v_{rh} \quad \Rightarrow \quad v_r^{(0)} = v_{rh}^{(0)} \quad , \quad v_r^{(1)} = v_{rh}^{(1)} \quad (3.71)$$

$$v_z = v_{zh} \quad \Rightarrow \quad v_z^{(0)} = v_{zh}^{(0)} \quad , \quad v_z^{(1)} = v_{zh}^{(1)} \quad (3.72)$$

From the equations (3.21) and (3.22) it is found that :

$$p^{(0)}(r,z,t) = p^{(0)}(r,t) \quad ; \quad p^{(1)}(r,z,t) = p^{(1)}(r,t) \quad (3.73)$$

In a first order approximation, the pressure in the fluid film is no function of the z-coordinate :

$$p = p(r,t) \quad (3.74)$$

Integration of differential equation (3.18) and (3.19), using boundary condition (3.69) and (3.71), yields :

$$\begin{aligned} v_r^{(0)} &= \frac{1}{2} \frac{\partial p^{(0)}}{\partial r} (z - g)(z - (g-h)) + \frac{g - z}{h} v_{rh}^{(0)} \\ v_r^{(1)} &= \frac{1}{2} \frac{\partial p^{(1)}}{\partial r} (z - g)(z - (g-h)) + \frac{g - z}{h} v_{rh}^{(1)} \end{aligned} \quad (3.75)$$

In a first order approximation, the radial velocity profile is the summation of a Poiseuille profile, as a result of the pressure gradient, and a Couette profile, as a result of the fluid velocity at the interface v_{rh} :

$$v_r = \frac{1}{2} \frac{\partial p}{\partial r} (z - g)(z - (g-h)) + \frac{g - z}{h} v_{rh} \quad (3.76)$$

Substitution of $v_r^{(0)}$ into the balance of mass and successive integration from $(g-h)$ to z , using boundary condition (3.72) yields :

(3.77):

$$\begin{aligned} v_z^{(0)} &= -\frac{1}{r} \frac{\partial}{\partial r} \left\{ \frac{1}{6} r \frac{\partial p^{(0)}}{\partial r} (z-g+h)(z^2 + (\frac{1}{2}h-2g)z + (g-h)(g+\frac{1}{2}h)) \right\} \\ &\quad - \frac{1}{r} \frac{\partial}{\partial r} \left\{ -\frac{1}{2} r v_{rh}^{(0)} \left(\frac{(z-g+h)(z-g-h)}{h} \right) \right\} + v_{zh}^{(0)} \end{aligned}$$

In the same way $v_z^{(1)}$ is calculated. Adding $\alpha v_z^{(1)}$ and $v_z^{(0)}$ yields a first order approximation of the axial fluid velocity v_z . Substitution of boundary condition (3.70) into v_z yields the Reynolds-equation for the fluid film in $V(t)$, the pressure gradient, $h(t)$ and the unknowns v_{rh} and v_{zh} :

$$-V(t) = v_{zh} + \frac{1}{r} \frac{\partial}{\partial r} \left(\frac{1}{12} r h^3 \frac{\partial p}{\partial r} - \frac{1}{2} r h v_{rh} \right) \quad (3.78)$$

3.4.3. Equations of motion for the biphasic mixture

In the preceding section the fluid velocity at the squeeze film side of the interface was assumed to be equal to :

$$\vec{v} = v_{rh} \vec{e}_r + v_{zh} \vec{e}_z \quad (3.79)$$

This section will start with the same assumption.

After scaling, a power series in α will be substituted in both the equation of motion and the boundary conditions. With the resulting equations v_r and v_z will be determined. Finally v_{rh} and v_{zh} will be obtained by matching the solution for the squeeze film via the boundary conditions to the solution for the mixture.

Equations of motion

In chapter 2, the equations of motion for a mixture are derived. Since u and v^s are equal to 0 for a rigid mixture, the equations of motion reduce drastically.

The balance of mass (2.42) becomes :

$$\frac{1}{r} \frac{\partial (r v_r)}{\partial r} + \frac{\partial v_z}{\partial z} = 0 \quad (3.80)$$

The equation of motion for the solid (2.43) can be dropped. The equations of motion for the interstitial fluid (2.44) become :

(3.81):

$$-n^f \frac{\partial p}{\partial r} + \frac{1}{3} \eta_a \frac{\partial}{\partial r} \left(\frac{v_r}{r} + \frac{\partial v_r}{\partial r} + \frac{\partial v_z}{\partial z} \right) + \eta_a \frac{\partial}{\partial r} \left(\frac{v_r}{r} + \frac{\partial v_r}{\partial r} \right) + \eta_a \frac{\partial^2 v_r}{\partial z^2} - K v_r = 0$$

(3.82):

$$-n^f \frac{\partial p}{\partial z} + \frac{1}{3} \eta_a \frac{\partial}{\partial z} \left(\frac{v_r}{r} + \frac{\partial v_r}{\partial r} + \frac{\partial v_z}{\partial z} \right) + \eta_a \frac{1}{r} \frac{\partial}{\partial r} \left(r \frac{\partial v_z}{\partial r} \right) + \eta_a \frac{\partial^2 v_z}{\partial z^2} - K v_z = 0$$

The equations are scaled in the same way as shown in § 3.2.2. Only results will be given here :

(3.83):

$$\frac{1}{r} \frac{\partial (r v_r)}{\partial r} + \frac{\partial v_z}{\partial z} = 0$$

(3.84):

$$-n^f \frac{\partial p}{\partial r} + \frac{4}{3} \frac{\eta_a}{\eta_f} \alpha^2 \frac{\partial}{\partial r} \left(\frac{v_r}{r} + \frac{\partial v_r}{\partial r} \right) + \frac{1}{3} \frac{\eta_a}{\eta_f} \alpha^2 \frac{\partial}{\partial r} \left(\frac{\partial v_z}{\partial z} \right) + \frac{\eta_a}{\eta_f} \frac{\partial^2 v_r}{\partial z^2} - \frac{K h_0^2}{\eta_f} v_r = 0$$

(3.85):

$$-n^f \frac{\partial p}{\partial z} + \frac{1}{3} \frac{\eta_a}{\eta_f} \alpha^2 \frac{\partial}{\partial z} \left(\frac{v_r}{r} + \frac{\partial v_r}{\partial r} \right) + \frac{4}{3} \frac{\eta_a}{\eta_f} \alpha^2 \frac{\partial^2 v_z}{\partial z^2} + \frac{\eta_a}{\eta_f} \alpha^4 \frac{1}{r} \frac{\partial}{\partial r} \left(r \frac{\partial v_z}{\partial r} \right) - \frac{K h_0^2}{\eta_f} \alpha^2 v_z = 0$$

The dependent variables are expanded into power series in terms of α :

$$p(r, z, t) = p^{(0)}(r, z, t) + p^{(1)}(r, z, t) \alpha + p^{(2)}(r, z, t) \alpha^2 + \dots, \quad (3.86)$$

$$v_r(r, z, t) = v_r^{(0)}(r, z, t) + v_r^{(1)}(r, z, t) \alpha + v_r^{(2)}(r, z, t) \alpha^2 + \dots, \quad (3.87)$$

$$v_z(r, z, t) = v_z^{(0)}(r, z, t) + v_z^{(1)}(r, z, t) \alpha + v_z^{(2)}(r, z, t) \alpha^2 + \dots, \quad (3.88)$$

where α equals h_0/R_0 , $\alpha \ll 1$.

Substituting the power series into the differential equations mentioned above, and collecting terms of equal power in α yields differential equations in the coefficients of the substituted power series (see § 3.2.2) :

balance of mass (3.83):

$$\frac{1}{r} \frac{\partial(rv_r^{(0)})}{\partial r} + \frac{\partial v_z^{(0)}}{\partial z} = 0 \quad (3.89)$$

$$\frac{1}{r} \frac{\partial(rv_r^{(1)})}{\partial r} + \frac{\partial v_z^{(1)}}{\partial z} = 0 \quad (3.90)$$

balance of momentum in r-direction (3.84):

$$-n^f \frac{\eta_f}{\eta_a} \frac{\partial p^{(0)}}{\partial r} + \frac{\partial^2 v_r^{(0)}}{\partial z^2} - \frac{Kh_0^2}{\eta_a} v_r^{(0)} = 0 \quad (3.91)$$

$$-n^f \frac{\eta_f}{\eta_a} \frac{\partial p^{(1)}}{\partial r} + \frac{\partial^2 v_r^{(1)}}{\partial z^2} - \frac{Kh_0^2}{\eta_a} v_r^{(1)} = 0 \quad (3.92)$$

balance of momentum in z-direction (3.85):

$$\frac{\partial p^{(0)}}{\partial z} = 0 \quad (3.93)$$

$$\frac{\partial p^{(1)}}{\partial z} = 0 \quad (3.94)$$

A first order approximation is found by neglecting higher order terms in α (order α^2 and higher), which is permitted since $\alpha \ll 1$, thus :

$$\frac{\partial v_z}{\partial z} = -\frac{1}{r} \frac{\partial(rv_r)}{\partial r} \quad (3.95)$$

$$\frac{\partial p}{\partial z} = 0 \quad (3.96)$$

$$-n^f \frac{\eta_f}{\eta_a} \frac{\partial p}{\partial r} + \frac{\partial^2 v_r}{\partial z^2} - \frac{Kh_0^2}{\eta_a} v_r = 0 \quad (3.97)$$

Boundary conditions

Before equation (3.97) can be solved, the boundary conditions (2.50) to (2.57) have to be scaled and have to be reduced by means of power series substitution.

Since the mixture is rigid, the boundary conditions (2.52), (2.53), and (2.56) will be dropped.

At the interface between the mixture and the rigid support, the following *kinematic boundary conditions* are valid :

$$v_r(r, z=0, t) = 0 \quad (3.98)$$

$$v_z(r, z=0, t) = 0 \quad (3.99)$$

At the interface between the squeeze film and the mixture both kinematic and dynamic boundary conditions are formulated :

kinematic boundary conditions,

$$n^f (v_r)_{z=(g-h)^-} = (v_r)_{z=(g-h)^+} \quad (3.100)$$

$$n^f (v_z)_{z=(g-h)^-} = (v_z)_{z=(g-h)^+} \quad (3.101)$$

dynamic boundary conditions,

$$\eta_a \left(-\frac{1}{3} \frac{1}{r} \frac{\partial(rv_r)}{\partial r} + \frac{2}{3} \frac{\partial v_z}{\partial z} \right)_{z=(g-h)^-} = n^f \eta_f \left(\frac{\partial v_z}{\partial z} \right)_{z=(g-h)^+} \quad (3.102)$$

$$\eta_a \left(\frac{\partial v_r}{\partial z} + \frac{\partial v_z}{\partial r} \right)_{z=(g-h)^-} = n^f \eta_f \left(\frac{\partial v_r}{\partial z} + \frac{\partial v_z}{\partial r} \right)_{z=(g-h)^+} \quad (3.103)$$

Rewriting and scaling the kinematic boundary conditions yields :

$$v'_r (r', z'=0, t') = 0 \quad (3.104)$$

$$v'_z (r', z'=0, t') = 0 \quad (3.105)$$

$$(v'_r)_{z'=(g'-h)'} = \frac{v'_{rh}}{n^f} \quad (3.106)$$

$$(v'_z)_{z'=(g'-h)'} = \frac{v'_{zh}}{n^f} \quad (3.107)$$

(accents will be left out from now on).

The scaled dynamic boundary conditions are given by :

$$\frac{\eta_a}{\eta_f} \left(\frac{\partial v_z}{\partial z} \right)_{z=(g-h)'} = n^f \left(\frac{\partial v_z}{\partial z} \right)_{z=(g-h)'} \quad (3.108)$$

$$\frac{\eta_a}{\eta_f} \left(\frac{\partial v_r}{\partial z} + \alpha^2 \frac{\partial v_z}{\partial r} \right)_{z=(g-h)'} = n^f \left(\frac{\partial v_r}{\partial z} + \alpha^2 \frac{\partial v_z}{\partial r} \right)_{z=(g-h)'} \quad (3.109)$$

where the balance of mass was substituted into (3.102). Since $\alpha \ll 1$, boundary condition (3.109) is in a first order approximation equal to :

$$\frac{\eta_a}{\eta_f} \left(\frac{\partial v_r}{\partial z} \right)_{z=(g-h)'} = n^f \left(\frac{\partial v_r}{\partial z} \right)_{z=(g-h)'} \quad (3.110)$$

Formally, this can be proven by means of power series substitution.

Solving the equations

Before equation (3.97) is solved, three new dimensionless variables will be introduced :

$$\beta = \frac{h_0}{H_0} \quad (3.111)$$

$$\eta = \frac{(n^f)^2 \eta_f}{\eta_a} \quad (3.112)$$

$$\delta = \sqrt{\frac{\eta_a}{KH_0^2}} \quad (3.113)$$

β is the ratio between the initial fluid film thickness and the mixture thickness, η is the ratio between the fluid film viscosity and the viscosity of the interstitial fluid, weighted by the reciprocal squared porosity, and δ is the ratio between the effect of the viscosity and the effect of the drag, which is exerted on the interstitial fluid by the solid. These parameters are introduced to obtain a relatively simple representation of the equations for the radial and axial fluid velocity (v_r and v_z) in the mixture. Moreover, during interpretation of the results only three parameters have to be varied.

Using these parameters, equation (3.97) becomes :

$$\frac{\partial v_r}{\partial z^2} - \frac{\beta^2}{\delta^2} v_r = \frac{\eta}{n^f} \frac{\partial p}{\partial r} \quad (3.114)$$

The solution of this differential equation is equal to :

$$v_r = c_1(r,t) e^{\frac{\beta}{\delta} z} + c_2(r,t) e^{-\frac{\beta}{\delta} z} - \frac{\eta}{n^f} \frac{\delta^2}{\beta^2} \frac{\partial p}{\partial r} \quad (3.115)$$

where the variables $c_1(r,t)$ and $c_2(r,t)$ have to be determined from the boundary conditions for v_r (3.104) and (3.106):

$$z = 0 \quad : \quad v_r = 0 \quad , \quad (3.116)$$

$$z = \frac{H_0}{h_0} = \frac{1}{\beta} \quad : \quad v_r = \frac{v_{rh}}{n^f} \quad . \quad (3.117)$$

The radial fluid velocity in the mixture v_r becomes :

(3.118):

$$v_r = \frac{1}{n^f} \left(v_{rh} + \eta \left(1 - e^{\frac{1}{\delta}} \right) \frac{\delta^2}{\beta^2} \frac{\partial p}{\partial r} \right) \frac{\sinh\left(\frac{\beta}{\delta} z\right)}{\sinh\left(\frac{1}{\delta}\right)} + \frac{\eta}{n^f} \frac{\delta^2}{\beta^2} \frac{\partial p}{\partial r} \left(e^{\frac{\beta}{\delta} z} - 1 \right)$$

Variable v_{rh} has to be determined by matching the solution for the radial velocity in the squeeze film via the dynamic boundary condition (3.110) to the above mentioned solution for the radial velocity in the mixture.

Therefore both for the squeeze film and the interstitial fluid, the derivative of v_r to z has to be determined at the interface $z = (g-h)$. Next these derivatives are substituted into (3.110). Evaluation of the resulting equation leads to :

$$v_{rh} = - v_{rh}^*(h) \frac{\partial p}{\partial r} \quad (3.119)$$

where v_{rh}^* only depends on the squeeze film thickness :

(3.120):

$$v_{rh}^* = \frac{\frac{\eta \delta h}{\beta} \left(\cosh\left(\frac{1}{\delta}\right) - 1 \right) + \frac{1}{2} \eta h^2 \sinh\left(\frac{1}{\delta}\right)}{\frac{\beta}{\delta} h \cosh\left(\frac{1}{\delta}\right) + \eta \sinh\left(\frac{1}{\delta}\right)}$$

For a rigid plate and a rigid plane mixture the film thickness is only a function of t :

$$h = h(t) \quad (3.121)$$

If a deformable mixture is investigated or the plate is replaced by e.g. a sphere, the film thickness will also become a function of r . This results in more complex calculations because v_{rh}^* and v_{zh}^* will become implicit functions of r in those cases.

To solve the Reynolds-equation for the squeeze film (3.78) independently of the equations of motion for the mixture, v_{zh} is required. This is done by integrating the balance of mass for the mixture from $z=0$ to H_0/h_0 under the boundary conditions (3.105) and (3.107):

$$z = 0 \quad : \quad v_z = 0 \quad , \quad (3.122)$$

$$z = \frac{H_0}{h_0} = \frac{1}{\beta} \quad : \quad v_z = \frac{v_{zh}}{n^f} \quad . \quad (3.123)$$

After some rearranging v_{zh} can be shown to be equal to :

$$v_{zh} = -v_{zh}^*(h(t)) \frac{1}{r} \frac{\partial}{\partial r} \left(r \frac{\partial p}{\partial r} \right) \quad (3.124)$$

where v_{zh}^* only depends on the squeeze film thickness via v_{rh}^* :

$$v_{zh}^* = \left(\frac{-v_{rh}^* \delta}{\beta} + \frac{2\delta^3 \eta}{\beta^3} \right) \frac{\left(\cosh\left(\frac{1}{\delta}\right) - 1 \right)}{\sinh\left(\frac{1}{\delta}\right)} - \frac{\delta^2 \eta}{\beta^3} \quad (3.125)$$

Now v_{rh} and v_{zh} are known, it is possible to solve the Reynolds-equation (3.78). Substituting v_{rh} and v_{zh} into (3.78) yields :

$$-V(t) = \left(-v_{zh}^* + \frac{h(t)}{2} v_{rh}^* + \frac{h^3(t)}{12} \right) \frac{1}{r} \frac{\partial}{\partial r} \left(r \frac{\partial p}{\partial r} \right) \quad (3.126)$$

At the right hand side of this equation, three terms from different origins can be distinguished, the first term is due to the fluid flux across the surface, the second term results from the additional radial fluid flux due to the radial velocity on the interface, and the third term represents the effect of the radial fluid flux due to the pressure gradient in the fluid film gap.

3.4.4. Film thickness and pressure distribution over the squeeze film

Integration of the Reynolds-equation (3.126) from 0 to r and subsequently from r to 1 with two boundary conditions for the pressure :

$$r = 1 : p(r, t) = 0 \quad (3.127)$$

$$r = 0 : \frac{\partial p}{\partial r} = 0 , \quad (3.128)$$

yields :

$$p(r, t) = \frac{3V(t)}{h^3 + 6 h v_{rh}^* - 12v_{zh}^*} (1 - r^2) \quad (3.129)$$

The relation between the film thickness and the velocity of the upper plate and the relation between the load and the pressure distribution complete the system of equations which has to be solved :

$$\begin{aligned} p(r, t) &= \frac{3V(t)}{h^3(t) + 6 h(t) v_{rh}^* - 12v_{zh}^*} (1 - r^2) \\ v_{rh}^* &= v_{rh}^*(h(t)) \\ v_{zh}^* &= v_{zh}^*(h(t)) \\ h(t) &= 1 - \int_0^t V(\tau) d\tau \\ F(t) &= 2 \int_0^1 p(r, t) r dr \end{aligned} \quad (3.130)$$

The load on the upper plate $F(t)$ will be prescribed.

By integrating the pressure distribution over the load carrying area, the system of equations (3.130) can be rewritten as :

$$F(t) = \frac{3}{2} \frac{V(t)}{h^3(t) + 6h(t)v_{rh}^* - 12v_{zh}^*} \quad (3.131)$$

$$\text{with :} \quad h(t) = 1 - \int_0^t V(\tau) d\tau$$

$$v_{rh}^* = v_{rh}^*(h(t)) \quad (3.120)$$

$$v_{zh}^* = v_{zh}^*(h(t)) \quad (3.125)$$

The pressure distribution appears to be :

$$p(r,t) = 2F(t)(1 - r^2) \quad \text{for } r \leq 1 \quad (3.132)$$

Substitution of (3.132) in (3.119) and (3.124) yields :

$$v_{rh} = 4 F(t) v_{rh}^* r \quad \text{for } r \leq 1 \quad (3.133)$$

$$v_{zh} = 8 F(t) v_{zh}^* \quad \text{for } r \leq 1 \quad (3.134)$$

3.4.5. Results

In accordance with the two preceding special cases, a stepload ($F(t) = 0$ for $t < 0$ and $F(t) = 1$ for $t \geq 0$) is applied to the upper plate. The pressure distribution over the fluid film (shown in figure 13) is equal to the pressure distribution for the plate-plate configuration.

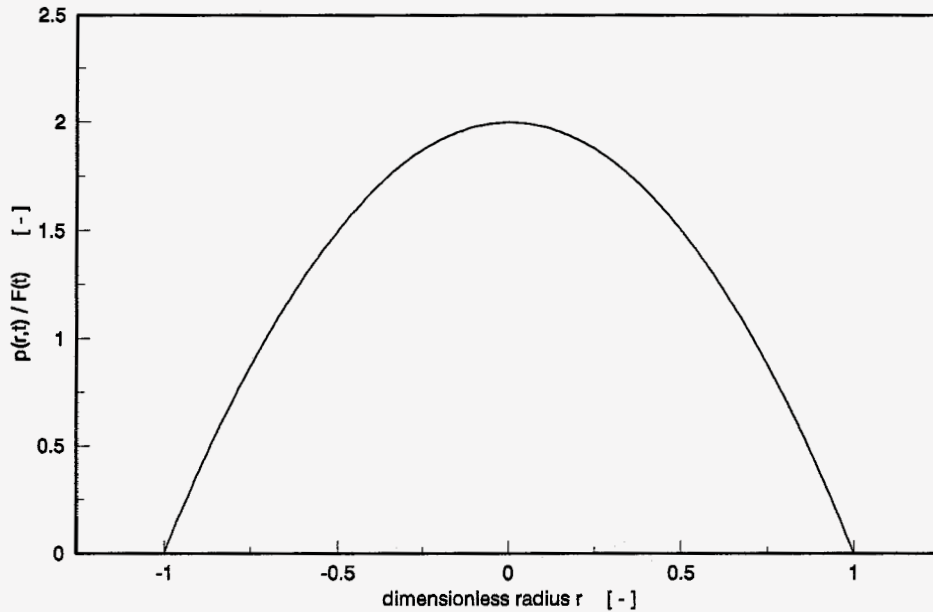


figure 13 The dimensionless pressure distribution (divided by the dimensionless load $F(t)$) over the fluid film

Equation (3.131) is solved numerically (see appendix II.2.3) for several values for the parameters δ and β . Because η depends on the apparent viscosity of the interstitial fluid η_a and no value is currently available for η_a , η is chosen to be equal to 1.0 .

figure 14 shows the calculated film thickness $h(t)$ versus time for four different values of δ (1.0, 0.1, 0.01, and 0.001), while $\beta = 1.0$ (thus the initial film thickness $h(0)$ being equal to the mixture thickness H_0), and $\eta = 1.0$. From this figure it can be seen that the smaller δ gets, the more $h(t)$ approaches the solution for the plate-plate configuration (see also figure 6). If δ is small, the drag in the mixture is very high as a result of a low permeability.

figure 15 shows the radial velocity profile immediately after application of the step load, for three different values of δ (1.0, 0.1, and 0.01), while $\beta = 1.0$ and $\eta = 1.0$.

For $\delta = 0.01$, corresponding to a low permeability of the mixture, there is almost no flow through the mixture ($v_{rh}^* \approx 0$ and $v_{zh}^* \approx 0$: figure 16 and figure 17), so the velocity profile in the gap approaches a parabolic velocity profile, which is found for a squeeze film between two rigid impermeable plates. In that case, equation (3.131) can be transformed into (3.45). For increasing δ ($\beta = 1.0$, $\eta = 1.0$), corresponding to increasing permeability of the mixture, the fluid flow in the mixture becomes more important. Besides through the gap between the upper plate and the mixture, the fluid can also escape through the mixture. This results in a faster decrease of $h(t)$ with time down to 0.

For $\delta = 0.1$ ($\beta = 1.0$, $\eta = 1.0$), a nearly uniform velocity profile can be seen in the center area of the mixture. In this area the viscosity of the interstitial fluid is apparently not important. However, near the surfaces of the mixture there are boundary layers as a result of viscous interaction of the interstitial fluid.

For $\delta = 1.0$ ($\beta = 1.0$, $\eta = 1.0$), the viscosity of the interstitial fluid is important in the whole mixture. The radial velocity profile is almost parabolic, as if no mixture is present.

figure 16 shows v_{rh}^* versus the film thickness $h(t)$. The radial fluid velocity at the fluid film - mixture interface v_{rh} is proportional to v_{rh}^* and linearly depends on the radius r (3.133).

For increasing δ , v_{rh}^* increases, which results in an increasing additional radial flow through the gap. v_{rh}^* decreases with decreasing $h(t)$ down to 0.

figure 17 shows v_{zh}^* versus the film thickness $h(t)$. The axial fluid velocity at the fluid film - mixture interface v_{zh} is proportional to v_{zh}^* and is independent of the radius r (3.134), forming a uniform axial velocity profile at the interface. v_{zh}^* (and thus v_{zh}) is negative, so the fluid penetrates the mixture. For increasing δ , the absolute value of v_{zh}^* increases, corresponding to an increasing flow into the mixture. As the axial velocity component across the interface v_{zh} is not equal to 0, even if $h(t)$ approximates to 0, the upper plate approaches the mixture with a finite velocity $V(t) > 0$.

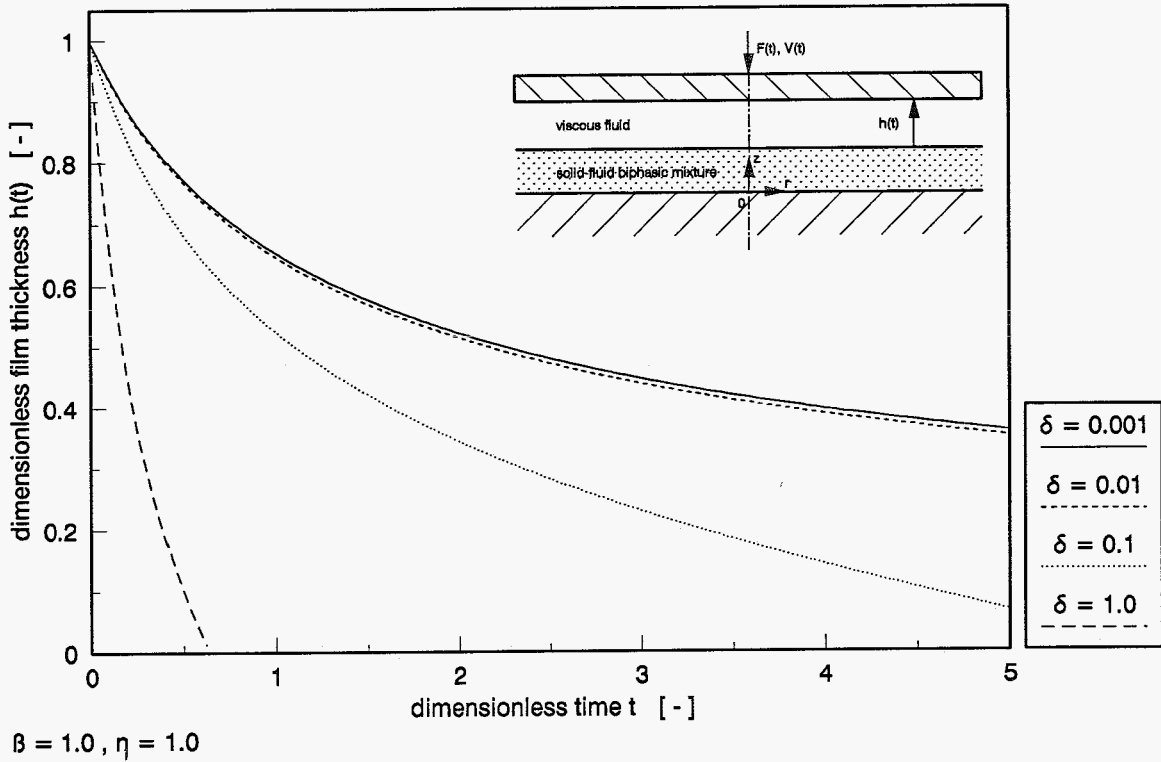


figure 14 The dimensionless film thickness $h(t)$ versus time, when a stepload is applied to the upper plate at $t=0$

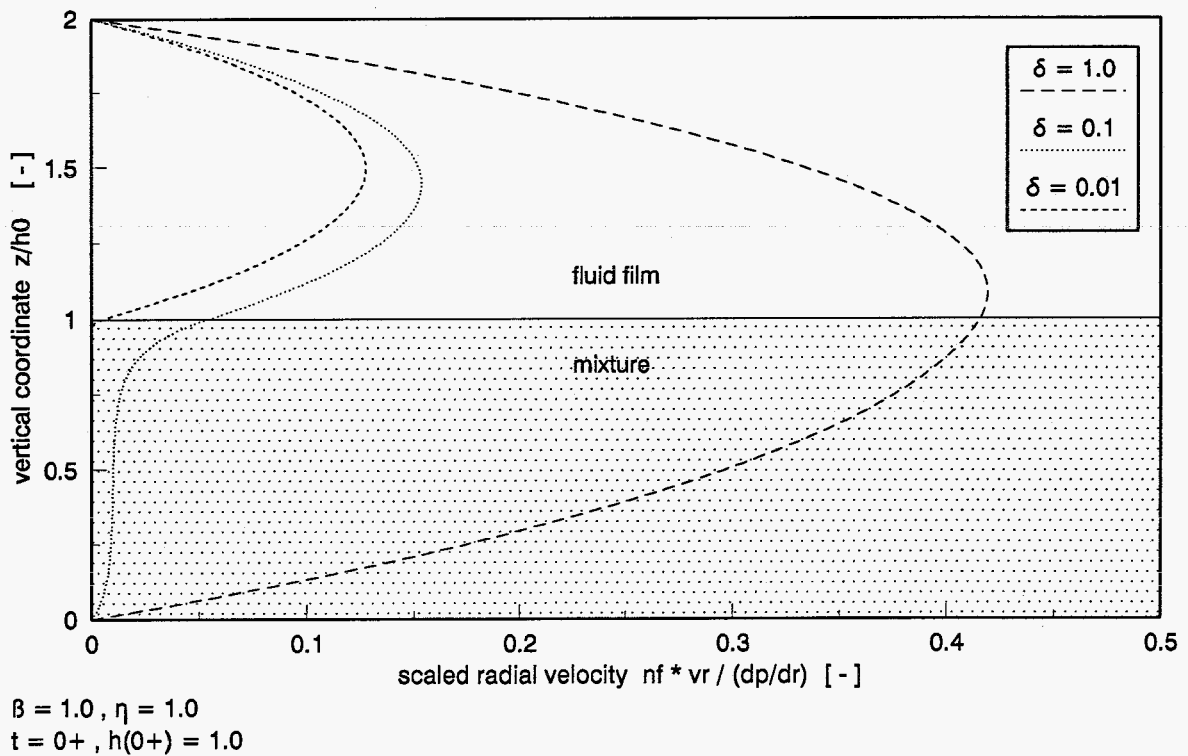


figure 15 Radial velocity profile at $t=0^+$ for $\beta = 1.0, \eta = 1.0$ and $\delta = 1.0, 0.1,$ and 0.01

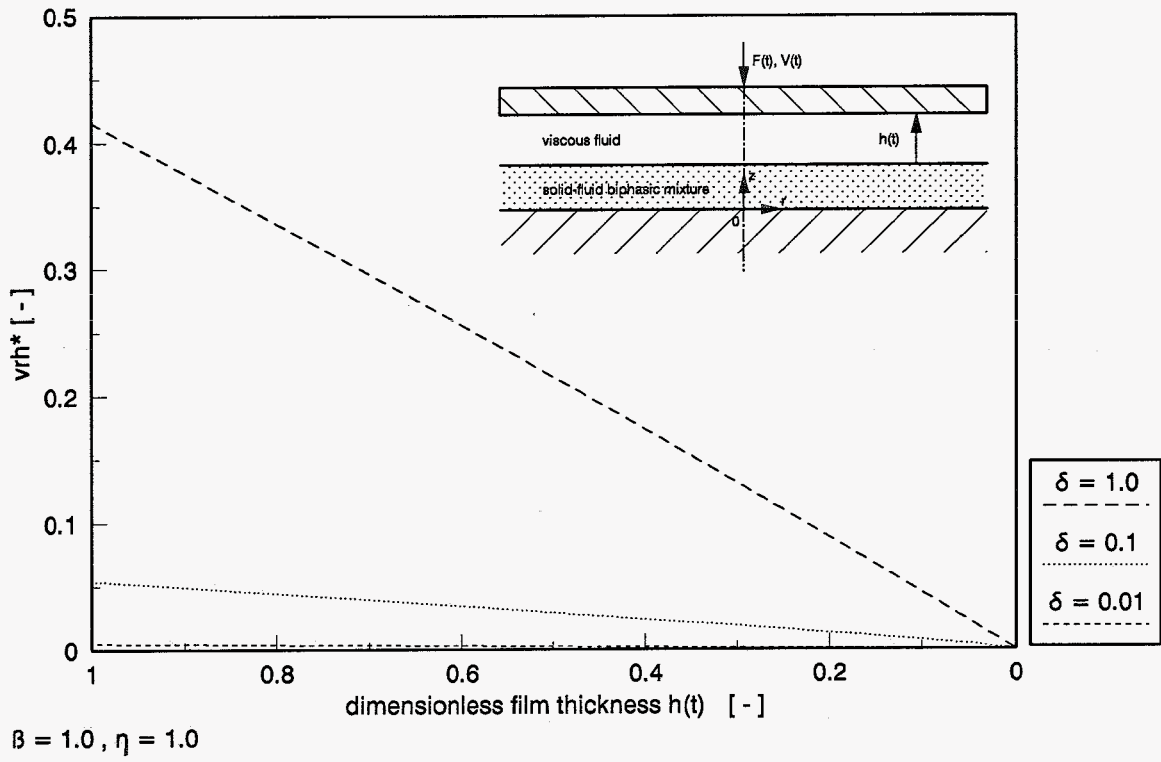


figure 16 v_{rh}^* as function of the dimensionless film thickness $h(t)$

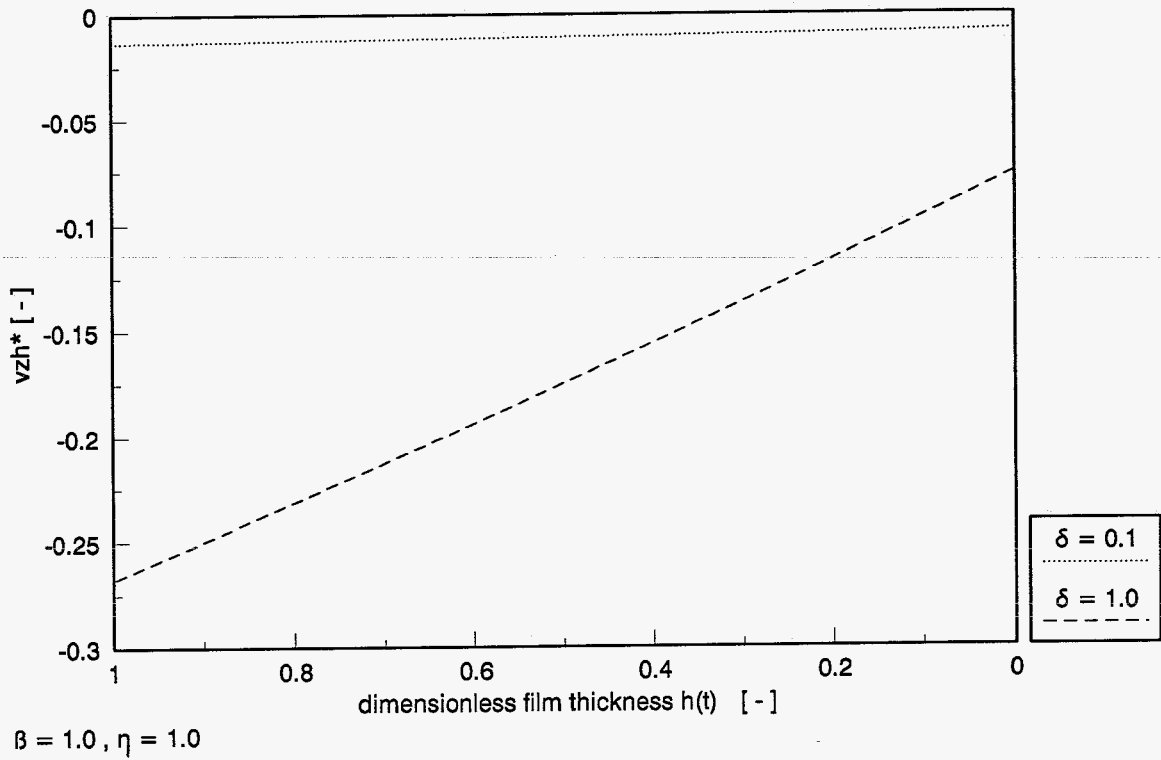


figure 17 v_{zh}^* as function of the dimensionless film thickness $h(t)$

Also the parameter β , the ratio between the film thickness h_0 and the mixture thickness H_0 , has a great influence on the upper plate velocity.

figure 18 shows the calculated film thickness $h(t)$ versus time for two different values β (1.0 and 0.1), while $\delta = 0.01$, and $\eta = 1.0$. When $\beta = 0.1$ (thus the mixture being 10 times as thick as the fluid film) it is relatively easy for the fluid to escape through the mixture, even though $\delta = 0.01$. This is primarily due to v_{zh} which increases considerably if β becomes smaller (figure 20 : $v_{zh}^* \approx 0$ for $\beta = 1.0$ and $\delta = 0.01$). Also v_m increases if β becomes smaller (figure 19). The influence of δ thus depends on β and vice versa.

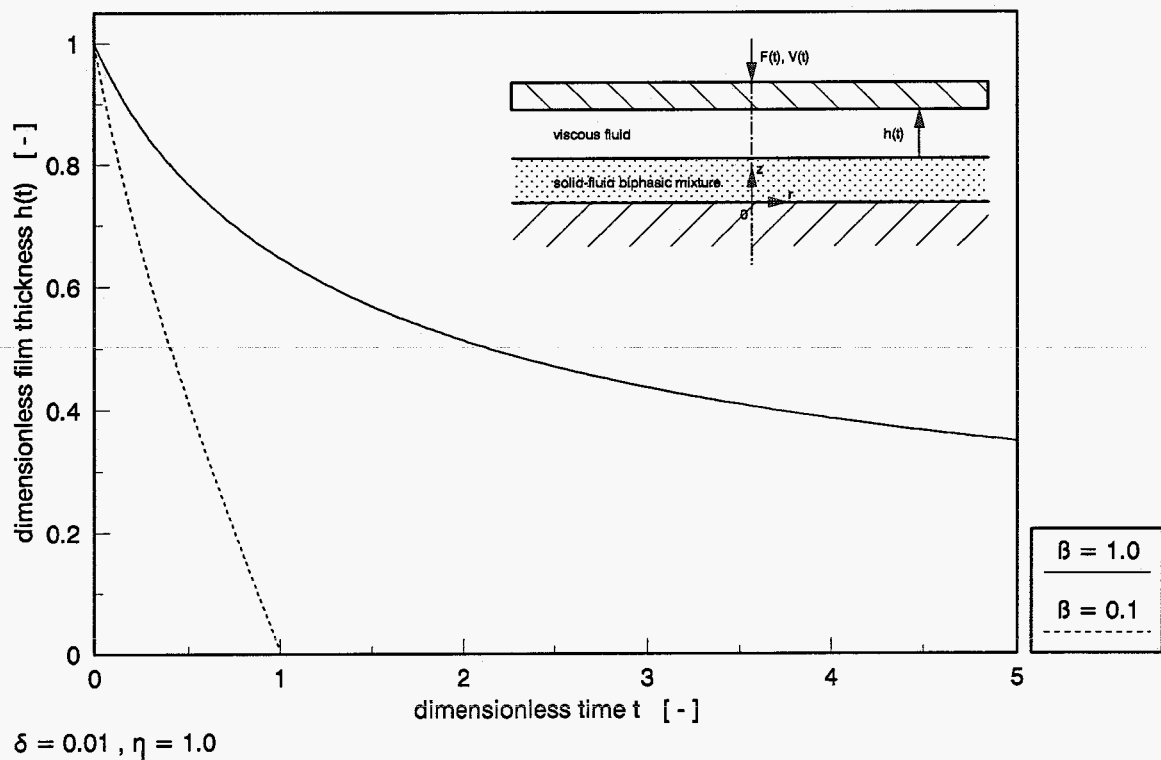


figure 18 The dimensionless film thickness $h(t)$ versus time, when a stepload is applied to the upper plate at $t=0$

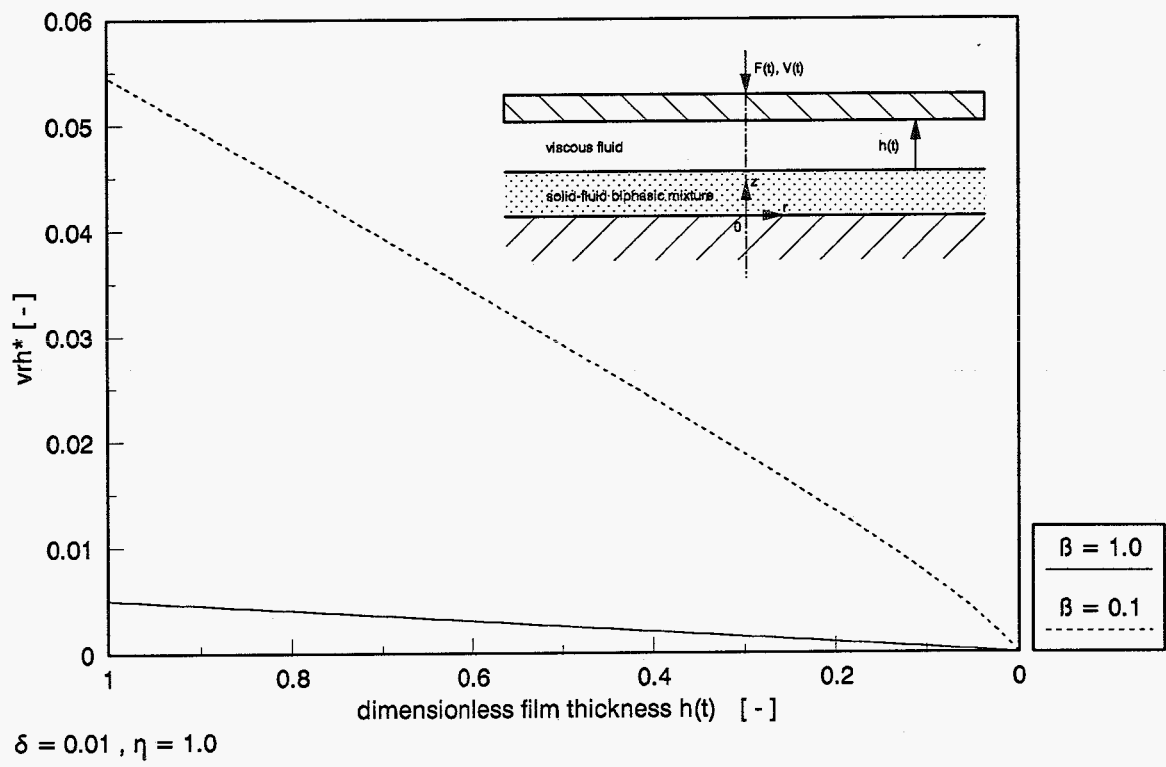


figure 19 v_{rh}^* as function of the dimensionless film thickness $h(t)$

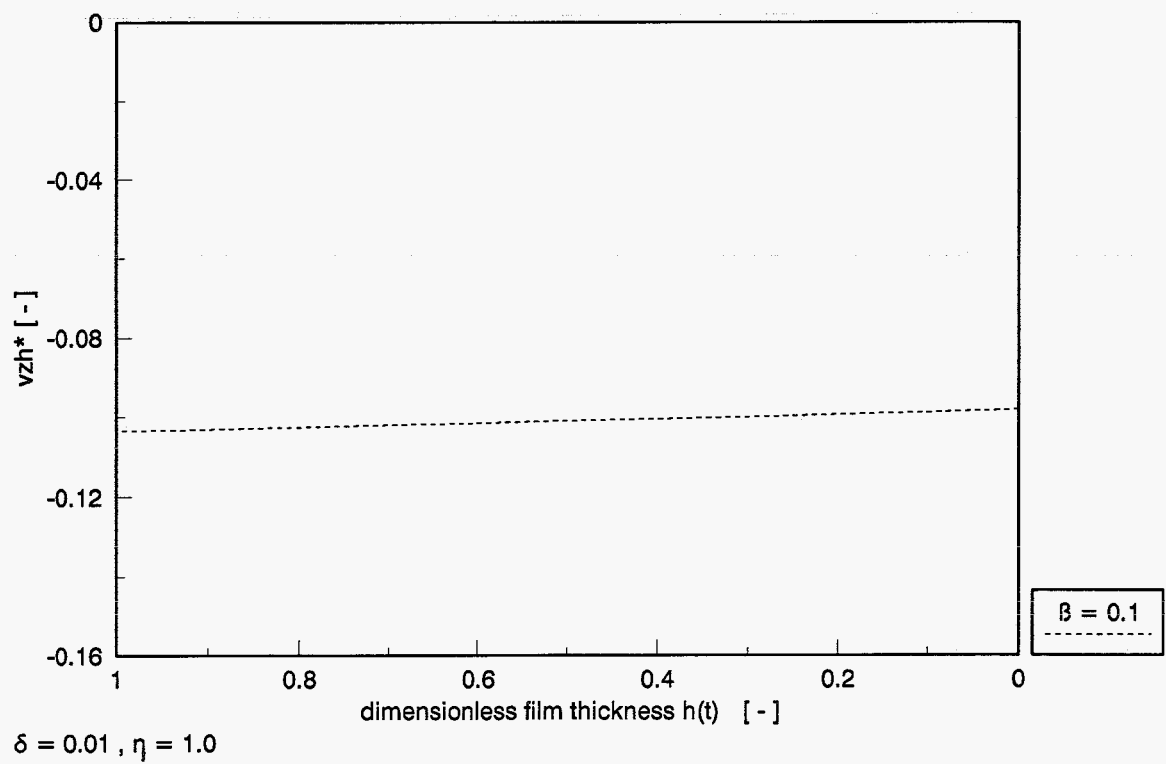


figure 20 v_{zh}^* as function of the dimensionless film thickness $h(t)$

Chapter 4. Conclusions and recommendations

In this report three special cases of Hou's squeeze film model for the human knee joint (Hou, 1989) have been investigated.

First a squeeze film between two rigid impermeable circular plates has been evaluated. This is called the reference case. As the plates approach, the resistance for the fluid to flow sideways increases, which results in a decreasing upper plate velocity with time. If the film thickness is approximately equal to 0, the upper plate velocity approximates to 0 too. In consequence of the load on the upper plate, a parabolic pressure profile is developed in the fluid film. Since the pressure gradient is maximal at the boundary of the plates, the radial flow is maximal there.

Next a squeeze film between a rigid spherical indenter and a rigid impermeable plane has been evaluated. The squeeze film does not last as long as in the reference case as a result of a strongly decreased resistance for the fluid to escape through the gap.

Yet the indenter velocity approximates to 0 if the film thickness approximates to 0, like in the reference case. The influence of a film thickness, which increases with the distance to the axis of symmetry, can easily be seen, since the pressure decreases faster with the radius than in the reference case. At the boundary of the load carrying area, the pressure gradient and the radial velocity are approximately equal to 0, which is in contrast with the reference case. The velocity profile in the gap is parabolic for both cases, since the fluid flows only as a result of a radial pressure gradient.

Finally a squeeze film between a circular flat plate and a rigid biphasic fluid-solid mixture has been evaluated. By means of the interface boundary conditions which were derived by Hou (1989), interaction between the fluid film and the interstitial fluid has been achieved. The number of boundary conditions appears to be sufficient for the system of equations for the squeeze film to be solved.

The influence of the mixture mainly depends on the permeability and porosity of the mixture, but also on the thickness of the mixture and the viscosity of the interstitial fluid. It is essential to take into account the viscosity of the interstitial fluid in order to allow interaction with the squeeze film fluid. The pressure distribution over the fluid film is not affected by the presence of a mixture and is actually the same as for the plate-plate configuration. The influence of the mixture onto the fluid film is entirely derived from the fluid velocity vector at the interface between mixture and fluid film, which results in a fluid flow across the interface (from film to mixture) and an additional radial flow through the gap. The radial velocity profile in the

gap can be described as an addition of a Poiseuille flow due to the pressure gradient and a Couette flow due to the radial velocity component of the fluid at the interface.

If the flow through the mixture contributes essentially to the decrease of the film thickness, the upper plate approaches the mixture with a finite velocity due to the axial fluid velocity component at the interface, which is directed from the fluid film to the mixture.

As in this report a rigid mixture is considered, it is obviously beforehand from the balance of mass, that the fluid has to penetrate the mixture. For the fluid in the mixture flows away sideways due to the pressure gradient, fluid has to be provided by the fluid film, since the mixture's volume does not change. Although the fluid appears to penetrate the mixture in this analysis, this does not necessarily have to occur in case of deformable mixtures.

It is recommended to continue this research by validating Hou's (1989) interface boundary conditions in experiments on a physical squeeze film model, which incorporates a rigid mixture. Because it may not be possible to perform experiments on a parallel squeeze film, a squeeze film between a spherical indenter and a rigid permeable biphasic fluid-solid mixture could be evaluated first.

Next a parameter study can be performed in order to choose a proper experimental set-up.

It may also be valuable to investigate the influence of a deformable mixture on the squeeze film. The mixture and thus the interface will probably deform due to the pressure gradient and the fluid flow through the mixture, which may influence the formulation of the interface boundary conditions.

References

Fung, Y.C., Foundations of solid mechanics. Prentice-Hall inc. Englewood Cliffs, New Jersey, 1965.

Gross, W.A., Matsch, L.A., Castelli, V., Eshel, A., Vohr, J.H., Wildmann, M., Fluid Film Lubrication. John Wiley & Sons, New York, 1980.

Hou, J.S., Formulation of synovial fluid-articular surface interface conditions, and asymptotic and numerical analyses of squeeze film lubrication of diarthrodial joints. PhD Thesis, Rensselaer Polytechnic Institute Troy, New York, 1989.

Hou, J.S., Holmes, M.H., Lai, W.M., Mow, V.C., Boundary conditions at the cartilage-synovial fluid interface for joint lubrication and theoretical verifications.

In: Journal of Biomechanical Engineering, ASME, Vol. 111 (1989). Pp. 78-87.

Lai, W.M., and Mow, V.C., Drag induced compression of articular cartilage during a permeation experiment.

In: Biorheology, Vol. 17 (1980). Pp. 111-123.

Lai, W.M., and Mow, V.C., Ultrafiltration of synovial fluid by cartilage.

In: Journal of the engineering mechanics division, ASCE, Vol. 104, No.EM1 (1978). Pp. 79-96.

McCutchen, C.W., Lubrication of Joints, in The Joints and Synovial Fluid (Volume I), edited by L. Sokoloff. Academic Press, New York, 1978.

Michell, A.G.M., Lubrication, Its principles and practice. Blackie & Son Limited, London and Glasgow, 1950.

Mow, V.C., The role of lubrication in biomechanical joints.

In: Journal of Lubrication Technology, ASME, Vol. 91 (1969), Pp. 320-329.

O'Conner, J.J., and Boyd, J., Standard handbook of lubrication engineering. McGraw-Hill Book Company, New York, 1968.

Oomens, C.W.J., A mixture approach to the mechanics of skin and subcutis.

PhD Thesis, Twente University of Technology, Twente, 1985.

Schreppers, G.J.M.A., Force transmission in the tibio-femoral contact complex.
PhD Thesis, Eindhoven University of Technology, Eindhoven, 1991.

Wismans, J., A three dimensional mathematical model of the human knee-joint.
PhD Thesis, Eindhoven University of Technology, Eindhoven, 1980.

Appendix I Vector identities

I.1. Vector identities in Cartesian coordinates

\vec{x} position vector $\vec{x}(x,y,z) = x\vec{e}_x + y\vec{e}_y + z\vec{e}_z$

\vec{v} velocity vector $\vec{v} = \dot{\vec{x}} = \dot{x}\vec{e}_x + \dot{y}\vec{e}_y + \dot{z}\vec{e}_z = v_x\vec{e}_x + v_y\vec{e}_y + v_z\vec{e}_z$

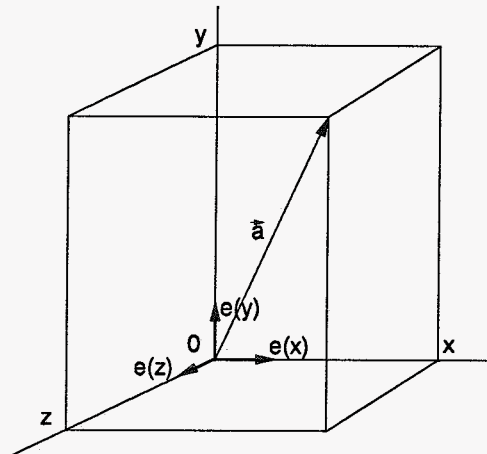


figure 21 Cartesian coordinate system

a scalar field $a(x,y,z)$

\vec{a} vector field $\vec{a}(x,y,z) = a_x\vec{e}_x + a_y\vec{e}_y + a_z\vec{e}_z$

$\vec{\nabla}$ gradient vector $\vec{\nabla}(x,y,z) = \vec{e}_x \frac{\partial}{\partial x} + \vec{e}_y \frac{\partial}{\partial y} + \vec{e}_z \frac{\partial}{\partial z}$

$$\text{grad}(a) = \vec{e}_x \frac{\partial a}{\partial x} + \vec{e}_y \frac{\partial a}{\partial y} + \vec{e}_z \frac{\partial a}{\partial z} \quad (\text{I.1})$$

$$\text{grad}(\vec{a}) = \quad (\text{I.2})$$

$$\vec{e}_x \left(\frac{\partial a_x}{\partial x} \vec{e}_x + \frac{\partial a_x}{\partial y} \vec{e}_y + \frac{\partial a_x}{\partial z} \vec{e}_z \right) + \vec{e}_y \left(\frac{\partial a_y}{\partial x} \vec{e}_x + \frac{\partial a_y}{\partial y} \vec{e}_y + \frac{\partial a_y}{\partial z} \vec{e}_z \right) + \vec{e}_z \left(\frac{\partial a_z}{\partial x} \vec{e}_x + \frac{\partial a_z}{\partial y} \vec{e}_y + \frac{\partial a_z}{\partial z} \vec{e}_z \right)$$

$$\text{div}(\vec{a}) = \vec{\nabla} \cdot \vec{a} = \frac{\partial a_x}{\partial x} + \frac{\partial a_y}{\partial y} + \frac{\partial a_z}{\partial z} \quad (\text{I.3})$$

$$\operatorname{div}(\operatorname{grad} a) = \vec{\nabla} \cdot (\vec{\nabla} a) = \frac{\partial^2 a}{\partial x^2} + \frac{\partial^2 a}{\partial y^2} + \frac{\partial^2 a}{\partial z^2} \quad (\text{I.4})$$

$$\operatorname{div}(\operatorname{grad} \vec{a}) = \vec{\nabla} \cdot (\vec{\nabla} \vec{a}) = \nabla^2 \vec{a} = \quad (\text{I.5})$$

$$\frac{\partial}{\partial x} \left(\frac{\partial a_x}{\partial x} \vec{e}_x + \frac{\partial a_x}{\partial y} \vec{e}_y + \frac{\partial a_x}{\partial z} \vec{e}_z \right) + \frac{\partial}{\partial y} \left(\frac{\partial a_y}{\partial x} \vec{e}_x + \frac{\partial a_y}{\partial y} \vec{e}_y + \frac{\partial a_y}{\partial z} \vec{e}_z \right) + \frac{\partial}{\partial z} \left(\frac{\partial a_z}{\partial x} \vec{e}_x + \frac{\partial a_z}{\partial y} \vec{e}_y + \frac{\partial a_z}{\partial z} \vec{e}_z \right)$$

$$\operatorname{grad}(\operatorname{div} \vec{a}) = \vec{\nabla} (\vec{\nabla} \cdot \vec{a}) =$$

$$\vec{e}_x \frac{\partial}{\partial x} \left(\frac{\partial a_x}{\partial x} + \frac{\partial a_y}{\partial y} + \frac{\partial a_z}{\partial z} \right) + \vec{e}_y \frac{\partial}{\partial y} \left(\frac{\partial a_x}{\partial x} + \frac{\partial a_y}{\partial y} + \frac{\partial a_z}{\partial z} \right) + \vec{e}_z \frac{\partial}{\partial z} \left(\frac{\partial a_x}{\partial x} + \frac{\partial a_y}{\partial y} + \frac{\partial a_z}{\partial z} \right) \quad (\text{I.6})$$

I.2. Vector identities in cylindrical coordinates

\vec{x} position vector $\vec{x}(r, \varphi, z) = r\vec{e}_r(\varphi) + z\vec{e}_z$

\vec{v} velocity vector $\vec{v} = \dot{\vec{x}} = \dot{r}\vec{e}_r + r\dot{\varphi}\vec{e}_\varphi + \dot{z}\vec{e}_z = v_r\vec{e}_r + v_\varphi\vec{e}_\varphi + v_z\vec{e}_z$

$$\dot{\vec{e}}_r = \dot{\varphi}\vec{e}_\varphi ; \quad \dot{\vec{e}}_\varphi = -\dot{\varphi}\vec{e}_r \quad (I.7)$$

$$\frac{\partial \vec{e}_r(\varphi)}{\partial \varphi} = \vec{e}_\varphi , \quad \frac{\partial \vec{e}_r(\varphi)}{\partial r} = 0 ; \quad \frac{\partial \vec{e}_\varphi}{\partial \varphi} = -\vec{e}_r , \quad \frac{\partial \vec{e}_\varphi}{\partial r} = 0 \quad (I.8)$$

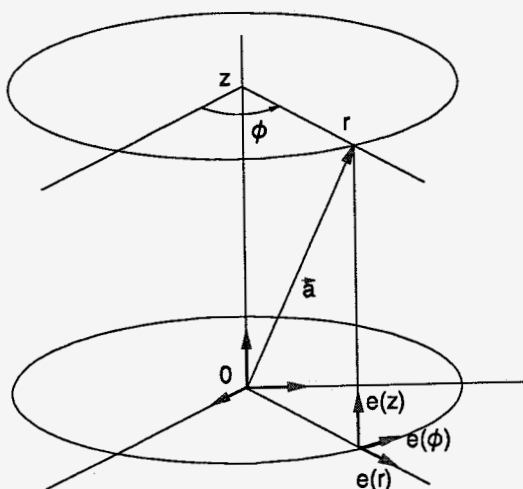


figure 22 Cylindrical coordinate system

a scalar field $a(r, \varphi, z)$

\vec{a} vector field $\vec{a}(r, \varphi, z) = a_r\vec{e}_r + a_\varphi\vec{e}_\varphi + a_z\vec{e}_z$

$\vec{\nabla}$ gradient vector $\vec{\nabla}(r, \varphi, z) = \vec{e}_r \frac{\partial}{\partial r} + \vec{e}_\varphi \frac{1}{r} \frac{\partial}{\partial \varphi} + \vec{e}_z \frac{\partial}{\partial z}$

$$\text{grad}(a) = \vec{e}_r \frac{\partial a}{\partial r} + \vec{e}_\varphi \frac{1}{r} \frac{\partial a}{\partial \varphi} + \vec{e}_z \frac{\partial a}{\partial z} \quad (\text{I.9})$$

$$\text{grad}(\vec{a}) = \quad (\text{I.10})$$

$$\begin{aligned} & \vec{e}_r \left(\frac{\partial a_r}{\partial r} \vec{e}_r + \left(\frac{1}{r} \frac{\partial a_r}{\partial \varphi} - \frac{1}{r} a_\varphi \right) \vec{e}_\varphi + \frac{\partial a_r}{\partial z} \vec{e}_z \right) + \vec{e}_\varphi \left(\frac{\partial a_\varphi}{\partial r} \vec{e}_r + \left(\frac{1}{r} \frac{\partial a_\varphi}{\partial \varphi} + \frac{1}{r} a_r \right) \vec{e}_\varphi + \frac{\partial a_\varphi}{\partial z} \vec{e}_z \right) + \\ & \vec{e}_z \left(\frac{\partial a_z}{\partial r} \vec{e}_r + \frac{1}{r} \frac{\partial a_z}{\partial \varphi} \vec{e}_\varphi + \frac{\partial a_z}{\partial z} \vec{e}_z \right) \end{aligned}$$

$$\text{div}(\vec{a}) = \vec{\nabla} \cdot \vec{a} = \frac{\partial a_r}{\partial r} + \frac{a_r}{r} + \frac{1}{r} \frac{\partial a_\varphi}{\partial \varphi} + \frac{\partial a_z}{\partial z} = \frac{1}{r} \frac{\partial(r a_r)}{\partial r} + \frac{1}{r} \frac{\partial a_\varphi}{\partial \varphi} + \frac{\partial a_z}{\partial z} \quad (\text{I.11})$$

$$\text{div}(\text{grad } a) = \vec{\nabla} \cdot (\vec{\nabla} a) = \nabla^2 a = \frac{\partial^2 a}{\partial r^2} + \frac{1}{r} \frac{\partial a}{\partial r} + \frac{1}{r^2} \frac{\partial^2 a}{\partial \varphi^2} + \frac{\partial^2 a}{\partial z^2} \quad (\text{I.12})$$

$$\text{div}(\text{grad } \vec{a}) = \vec{\nabla} \cdot (\vec{\nabla} \vec{a}) = \nabla^2 \vec{a} = \quad (\text{I.13})$$

$$\begin{aligned} & \frac{\partial}{\partial r} \left(\frac{\partial a_r}{\partial r} \vec{e}_r + \left(\frac{1}{r} \frac{\partial a_r}{\partial \varphi} - \frac{a_\varphi}{r} \right) \vec{e}_\varphi + \frac{\partial a_r}{\partial z} \vec{e}_z \right) + \\ & \frac{1}{r} \left(\left\{ \left(\frac{\partial a_r}{\partial r} - \frac{a_r}{r} \right) + \frac{\partial}{\partial \varphi} \left(\frac{\partial a_\varphi}{\partial r} - \frac{a_\varphi}{r} \right) \right\} \vec{e}_r + \left\{ \frac{\partial a_\varphi}{\partial r} + \frac{1}{r} \left(\frac{\partial a_r}{\partial \varphi} - a_\varphi \right) + \frac{1}{r} \frac{\partial}{\partial \varphi} \left(\frac{\partial a_\varphi}{\partial \varphi} + a_r \right) \right\} \vec{e}_\varphi + \right. \\ & \left. + \left\{ \frac{\partial a_r}{\partial z} + \frac{\partial^2 a_\varphi}{\partial \varphi \partial z} \right\} \vec{e}_z \right) + \frac{\partial}{\partial z} \left(\frac{\partial a_z}{\partial r} \vec{e}_r + \frac{1}{r} \frac{\partial a_z}{\partial \varphi} \vec{e}_\varphi + \frac{\partial a_z}{\partial z} \vec{e}_z \right) \end{aligned}$$

$$\text{grad}(\text{div } \vec{a}) = \vec{\nabla} (\vec{\nabla} \cdot \vec{a}) = \quad (\text{I.14})$$

$$\begin{aligned} & \vec{e}_r \frac{\partial}{\partial r} \left(\frac{1}{r} \frac{\partial(r a_r)}{\partial r} + \frac{1}{r} \frac{\partial a_\varphi}{\partial \varphi} + \frac{\partial a_z}{\partial z} \right) + \vec{e}_\varphi \frac{1}{r} \frac{\partial}{\partial \varphi} \left(\frac{1}{r} \frac{\partial(r a_r)}{\partial r} + \frac{1}{r} \frac{\partial a_\varphi}{\partial \varphi} + \frac{\partial a_z}{\partial z} \right) + \\ & \vec{e}_z \frac{\partial}{\partial z} \left(\frac{1}{r} \frac{\partial(r a_r)}{\partial r} + \frac{1}{r} \frac{\partial a_\varphi}{\partial \varphi} + \frac{\partial a_z}{\partial z} \right) \end{aligned}$$

Appendix II Turbo Pascal programs

II.1. Program to generate an input file

```
program Generate_Input_File;
{-----}
    The load on the upper plate is prescribed for a certain number
    of timesteps. A file is made in which the timebase and the load
    for each timestep will be put.
    A rampfunction is used to describe the load as a function of time:
        F(t) = t/T   for   t<=T
        F(t) = 1.0   for   t> T
    Three positions on top of the inputfile are reserved for:
        1. Total_Time
        2. Number_Of_Timesteps
        3. Time T (the time in which F grows from 0 to 1)
    The first column contains the time, the second the load F.
    -----}
uses crt,dos;

const n = 2000;           {maximum Number_Of_Timesteps}

var i,j                  : integer;
    Number_Of_Timesteps : integer;
    Total_Time,T,Time_Step : real;
    Input_File           : text;
    File_Name            : string[20];
    Dirinfo              : searchrec;
    Time_Base,Load       : array[0..n,0..0] of real;
{-----}
procedure Timebase;

var i:integer;

begin
    repeat write('Total Time           = ');
           readln(Total_Time);
    until Total_Time > 0;

    repeat write('T                   = ');
           readln(T);
    until T > 0;

    repeat write('Number_Of_Timesteps [1,n] = ');
           readln(Number_Of_Timesteps);
    until (Number_Of_Timesteps > 0) and (Number_Of_Timesteps <= n);

    Time_Step := Total_Time/Number_Of_Timesteps;
```

```

if T >= Total_Time then
  writeln('*** WARNING *** : T >= Total Time');

if T <= Time_Step then
  writeln('*** WARNING *** : T <= Time Step');

for i := 0 to Number_Of_Timesteps do
  begin
    Time_Base[i,0] := i*Time_Step;
  end;
end;
{-----}
procedure Load_Prescription;

var      i:integer;

begin
  for i := 0 to Number_Of_Timesteps do
    begin
      if Time_Base[i,0] <= T then Load[i,0] := Time_Base[i,0]/T;
      if Time_Base[i,0] > T then Load[i,0] := 1.0;
    end;
  end;
{-----}
procedure Write_Input_File;

begin
  j:=0;
  repeat
    write('File name for inputfile      = ');
    readln(File_Name);
    findfirst(File_Name,Archive,Dirinfo);
    if DosError = 0 then
      begin
        writeln('*** FILE ALREADY EXISTS ***');
        j:=j+1;
      end;
  until (DosError <> 0) or (j=3);
  if j<3 then
    begin
      assign(Input_File,File_Name);
      rewrite(Input_File);
      writeln(Input_File,Total_Time:12:6);
      writeln(Input_File,Number_Of_Timesteps);
      writeln(Input_File,T:12:6);
      for i := 0 to (Number_Of_Timesteps) do
        writeln(Input_File,Time_Base[i,0]:12:6,' ',Load[i,0]:12:6);
      close(Input_File);
    end
  else

```

```
begin
    writeln('*** PROGRAM TERMINATED ***');
    HALT;
end;
end;
```

```
{-----}
    Main Program
-----}
```

```
begin
    clrscr;
    Timebase;
    Load_Prescription;
    Write_Input_File;
end.
```

```
{-----}
```


II.2. Programs to calculate the squeeze film thickness

II.2.1. Two plates

```
program Two_Plates;
{-----}
  The squeeze film thickness is calculated given the load F on the
  upper plate for a certain number of timesteps.
  The inputfile has to meet the next lay-out:
  - Three positions on top of the inputfile have to contain:
      1. Total_Time
      2. Number_Of_Timesteps
      3. T (see input.pas).
  - The first column has to contain the time base, the second the
    load F.
  A three column outputfile is made; the first column contains the
  Timebase, the second the film thickness h and the third the upper
  plate velocity V.
{-----}
uses crt,dos;

const n      =      2000;      {maximum Number_Of_Timesteps}
      crit   =      1e-6;      {iteration criterion}

var i                : integer;
    Number_Of_Timesteps : integer;
    Total_Time,Time_Step,T : real;
    Input_File,Output_File : text;
    File_Name           : string[20];
    Dirinfo             : searchrec;
    Time_Base,Load      : array[0..n,0..0] of real;
    h_new,V_old,V_new   : array[0..n,0..0] of real;
{-----}
procedure Read_Input_File;      {Read Timebase and Load}

var i,j : integer;

begin
  i:=0;
  repeat
    write('File name for inputfile = ');
    readln(File_Name);
    findfirst(File_Name,Archive,Dirinfo);
    if DosError <> 0 then i:=i+1;
  until (DosError = 0) or (i=2);
  if i<2 then
    begin
      assign(Input_File,File_Name);
      reset(Input_File);
```

```

    readln(Input_File,Total_Time,Number_Of_Timesteps,T);
    for j:=0 to Number_Of_Timesteps do
        readln(Input_File,Time_Base[j,0],Load[j,0]);
    close(Input_File);
    Time_Step := Total_Time/Number_Of_Timesteps;
end
else
begin
    writeln('*** FILE NOT FOUND ***');
    HALT;
end;
end;
{-----}
procedure Write_Output_File;      {Write h and V}

var i,j : integer;

begin
    j:=0;
    repeat
        write('File name for outputfile = ');
        readln(File_Name);
        findfirst(File_Name,Archive,Dirinfo);
        if DosError = 0 then
            begin
                writeln('*** FILE ALREADY EXISTS ***');
                j:=j+1;
            end;
        until (DosError <> 0) or (j=3);
        if j<3 then
            begin
                assign(Output_File,File_Name);
                rewrite(Output_File);
                writeln(Output_File,Total_Time:12:6);
                writeln(Output_File,Number_Of_Timesteps);
                writeln(Output_File,T:12:6);
                for i := 0 to Number_Of_Timesteps do
                    writeln(Output_File,Time_Base[i,0]:12:6,' ',
                                h_new[i,0]:12:6,' ',
                                V_new[i,0]:12:6);
                close(Output_File);
            end
        else
            begin
                writeln('*** PROGRAM TERMINATED ***');
                HALT;
            end;
    end;
end;

```

```

{-----}
procedure Begin_Conditions;

begin

write('Initial dimensionless film thickness      : ');
readln(h_new[0,0]);
write('Initial dimensionless upper plate velocity : ');
readln(V_new[0,0]);

end;
{-----}
function Power(mantisse,exponent:real):real;

var help1 : real;

begin
  if (mantisse = 0) then Power := 0
  else
    if (exponent = 0) then Power := 1
    else
      if (mantisse > 0) then Power := exp((ln(mantisse))*exponent)
      else
        begin
          if (exponent-int(exponent)=0) and (odd(round(exponent))=true)
          then help1 := 1
          else help1 :=-1;
          Power := help1 * exp(ln(-mantisse) * exponent);
        end;
      end;
end;
{-----}
function fvcon(V,h,F:real):real; {relation between V and Load}

begin
  fvcon := (3/2)*(V/power(h,3))-F;
end;
{-----}
function derfvcon(h:real):real; {derivative to V of the relation
                                between V and Load}

begin
  derfvcon := (3/2)*(1/power(h,3));
end;

```

```

{-----}
procedure Iteration;           {Newton-Raphson iteration}

var help : real;

begin
  repeat
    help := (fvcon(V_old[i,0],h_new[i,0],Load[i,0])/derfvcon(h_new[i,0]));
    V_new[i,0] := V_old[i,0] - help;
    h_new[i,0] := h_new[i-1,0] - (1/2)*(V_new[i-1,0]+V_new[i,0])*Time_Step;
    V_old[i,0] := V_new[i,0];
  until (fvcon(V_new[i,0],h_new[i,0],Load[i,0]) < crit);
end;

{-----}
      Main Program
{-----}

begin
  clrscr;
  Read_Input_File;
  Begin_Conditions;
  for i := 1 to Number_Of_Timesteps do
    begin
      V_old[i,0] := V_new[i-1,0];
      h_new[i,0] := h_new[i-1,0];
      Iteration;
    end;
  Write_Output_File;
end.

{-----}

```

II.2.2. Spherical indenter - Plate

```
program Plate_Sphere;
{-----}
    The squeeze film thickness is calculated given the load F on the
    upper plate for a certain number of timesteps.
    The inputfile has to meet the next lay-out:
    - Three positions on top of the inputfile have to contain:
      1. Total_Time
      2. Number_Of_Timesteps
      3. T (see input.pas).
    - The first column has to contain the time base, the second the
      load F.
    A three column outputfile is made; the first column contains the
    Timebase, the second the film thickness h and the third the upper
    plate velocity V.
{-----}
uses    crt,dos;

const  n      =      1500;      {maximum Number_Of_Timesteps}
       crit   =      1e-6;      {iteration criterion}
       h00    =      0.1;      {minimal film thickness at t=0}
       R0     =      20;      {scalingfactor for radius r}
       Ri     =      50;      {radius of the sphere}

var    i      : integer;
       Number_Of_Timesteps : integer;
       Total_Time,Time_Step,T : real;
       Input_File,Output_File : text;
       File_Name           : string[20];
       Dirinfo             : searchrec;
       Time_Base,Load      : array[0..n,0..0] of real;
       h_new0,h_new1,V_old,V_new : array[0..n,0..0] of real;
{-----}
procedure Read_Input_File;      {Read Timebase and Load}
var    i,j : integer;

begin
    i:=0;
    repeat
        write('File name for inputfile = ');
        readln(File_Name);
        findfirst(File_Name,Archive,Dirinfo);
        i:=i+1;
    until (DosError = 0) or (i=2);
    if i<2 then
        begin
            assign(Input_File,File_Name);
            reset(Input_File);
            readln(Input_File,Total_Time,Number_Of_Timesteps,T);
```

```

    for j:=0 to Number_Of_Timesteps do
        readln(Input_File,Time_Base[j,0],Load[j,0]);
    close(Input_File);
    Time_Step := Total_Time/Number_Of_Timesteps;
end
else
begin
    writeln('*** FILE NOT FOUND ***');
    HALT;
end;
end;
end;
{-----}
procedure Write_Output_File;      {Write h and V}

var i,j : integer;

begin
    j:=0;
    repeat
        write('File name for outputfile = ');
        readln(File_Name);
        findfirst(File_Name,Archive,Dirinfo);
        if DosError = 0 then
            begin
                writeln('*** FILE ALREADY EXISTS ***');
                j:=j+1;
            end;
        until (DosError <> 0) or (j=3);
        if j<3 then
            begin
                assign(Output_File,File_Name);
                rewrite(Output_File);
                writeln(Output_File,Total_Time:12:6);
                writeln(Output_File,Number_Of_Timesteps);
                writeln(Output_File,T:12:6);
                for i := 0 to Number_Of_Timesteps do
                    writeln(Output_File,Time_Base[i,0]:12:6,' ',
                        h_new0[i,0]:12:6,' ',
                        V_new[i,0]:12:6);
                close(Output_File);
            end
        else
            begin
                writeln('*** PROGRAM TERMINATED ***');
                HALT;
            end;
        end;
    end;
end;
end;

```

```

{-----}
procedure Begin_Conditions;

begin

write('Initial minimal dimensionless film thickness : ');
readln(h_new0[0,0]);
write('Initial dimensionless upper plate velocity   : ');
readln(V_new[0,0]);

end;
{-----}
function Power(mantisse,exponent:real):real;

var help1 : real;

begin
  if (mantisse = 0) then Power := 0
  else
    if (exponent = 0) then Power := 1
    else
      if (mantisse > 0) then Power := exp((ln(mantisse))*exponent)
      else
        begin
          if (exponent-int(exponent)=0) and (odd(round(exponent))=true)
          then help1 := 1
          else help1 :=-1;
          Power := help1 * exp(ln(-mantisse) * exponent);
        end;
      end;
end;
{-----}
function fvcon(V,h0,h1,F:real):real; {relation between V and Load}

var help1:real;

begin
  fvcon := (3/2)*(V/(h0*sqr(h1)))-F;
  help1 := (3/2)*(V/(h0*sqr(h1)))-F;
end;
{-----}
function derfvcon(h0,h1:real):real; {derivative to V of the relation
                                     between V and Load}

var help2:real;
begin
  derfvcon := (3/2)*(1/(h0*sqr(h1)));
  help2:=(3/2)*(1/(h0*sqr(h1)));
end;

```



```

{-----}
procedure Iteration;           {Newton-Raphson iteration}

var help : real;

begin
  repeat
    help:=(fvcon(V_old[i,0],h_new0[i,0],h_new1[i,0],Load[i,0])/
             derfvcon(h_new0[i,0],h_new1[i,0]));
    V_new[i,0] := V_old[i,0] - help;
    h_new0[i,0] := h_new0[i-1,0] - (1/2)*(V_new[i-1,0]+V_new[i,0])*Time_Step;
    h_new1[i,0] := h_new0[i,0]+(1/2)*sqr(R0)/(Ri*h00);
    V_old[i,0] := V_new[i,0];
  until (fvcon(V_new[i,0],h_new0[i,0],h_new1[i,0],Load[i,0]) < crit);
end;

{-----}
Main Program
{-----}

begin
  clrscr;
  Read_Input_File;
  Begin_Conditions;
  for i := 1 to Number_Of_Timesteps do
    begin
      V_old[i,0] := V_new[i-1,0];
      h_new0[i,0] := h_new0[i-1,0];
      h_new1[i,0] := h_new0[i,0]+(1/2)*sqr(R0)/(Ri*h00);
      Iteration;
    end;
  Write_Output_File;
end.

{-----}

```

II.2.3. Plate - Mixture

```
program Plate_Mixture;
{-----}
    The squeeze film thickness is calculated given the load F on the
    upper plate for a certain number of timesteps.
    The inputfile has to meet the next lay-out:
    - Three positions on top of the inputfile have to contain:
      1. Total_Time
      2. Number_Of_Timesteps
      3. T (see input.pas).
    - The first column has to contain the time base, the second the
      load F.
    A three column outputfile is made; the first column contains the
    Timebase, the second the film thickness h and the third the upper
    plate velocity V.
    -----}
uses crt,dos;

const n = 2000; {maximum Number_Of_Timesteps}
      crit = 1e-6; {iteration criterion}
      delta = 0.1;
      beta = 1;
      eta = 1;

var i,Counter : integer;
    Number_Of_Timesteps : integer;
    Total_Time,Time_Step,T : real;
    help0,help1,help2,help3,help4 : extended;
    Input_File,Output_File : text;
    File_Name : string[20];
    Dirinfo : searchrec;
    Time_Base,Load : array[0..n,0..0] of real;
    h_new,V_old,V_new : array[0..n,0..0] of real;
{-----}
procedure Read_Input_File; {Read Timebase and Load}

var i,j : integer;

begin
    i:=0;
    repeat
        write('File name for inputfile = ');
        readln(File_Name);
        findfirst(File_Name,Archive,Dirinfo);
        if DosError <> 0 then i:=i+1;
    until (DosError = 0) or (i=2);
    if i<2 then
        begin
```

```

    assign(Input_File,File_Name);
    reset(Input_File);
    readln(Input_File>Total_Time,Number_Of_Timesteps,T);
    for j:=0 to Number_Of_Timesteps do
        readln(Input_File,Time_Base[j,0],Load[j,0]);
    close(Input_File);
    Time_Step := Total_Time/Number_Of_Timesteps;
end
else
begin
    writeln('*** FILE NOT FOUND ***');
    HALT;
end;
end;
{-----}
procedure Write_Output_File;      {Write h and V}

var i,j : integer;

begin
    j:=0;
    repeat
        write('File name for outputfile = ');
        readln(File_Name);
        findfirst(File_Name,Archive,Dirinfo);
        if DosError = 0 then
            begin
                writeln('*** FILE ALREADY EXISTS ***');
                j:=j+1;
            end;
        until (DosError <> 0) or (j=3);
        if j<3 then
            begin
                assign(Output_File,File_Name);
                rewrite(Output_File);
                writeln(Output_File>Total_Time:12:6);
                writeln(Output_File>Number_Of_Timesteps);
                writeln(Output_File>T:12:6);
                for i := 0 to Counter do
                    writeln(Output_File>Time_Base[i,0]:12:6,' ',
                                h_new[i,0]:12:6,' ',
                                V_new[i,0]:12:6);
                close(Output_File);
            end
        else
            begin
                writeln('*** PROGRAM TERMINATED ***');
                HALT;
            end;
    end;
end;

```

```

{-----}
procedure Begin_Conditions;

begin

write('Initial dimensionless film thickness      : ');
readln(h_new[0,0]);
write('Initial dimensionless upper plate velocity : ');
readln(V_new[0,0]);

end;
{-----}
function Power(mantisse,exponent:real):real;

var help : real;

begin
  if (mantisse = 0) then Power := 0
  else
    if (exponent = 0) then Power := 1
    else
      if (mantisse > 0) then Power := exp((ln(mantisse))*exponent)
      else
        begin
          if (exponent-int(exponent)=0) and (odd(round(exponent))=true)
          then help := 1
          else help :=-1;
          Power := help * exp(ln(-mantisse) * exponent);
        end;
      end;
end;
{-----}
function sinh(arg:real):extended;

begin
  sinh := (1/2)*(exp(arg)-exp(-arg));
end;
{-----}
function cosh(arg:real):extended;

begin
  cosh := (1/2)*(exp(arg)+exp(-arg));
end;
{-----}
function vrh(h:real):real;          {radial fluidvelocity at interface}

begin
  vrh := (help2*h+(1/2)*help4*sqr(h))/(help3*h+help4);
end;

```

```

{-----}
function vzh(h:real):real;          {axial fluidvelocity at interface}

var vzh1,vzh2 :extended;

begin
    vzh1 := ((-vrh(h)*delta/beta)+2*eta*power(delta,3)/power(beta,3));
    vzh2 := power(delta,2)*eta/power(beta,3);
    vzh  := (vzh1/help1)*(help0-1)-vzh2;
end;
{-----}
function fvcon(V,h,F,vrh,vzh:real):real;    {relation between V and load}

begin
    fvcon := (3/2)*(V/(power(h,3)+6*h*vrh-12*vzh))-F;
end;
{-----}
function derfvcon(h,vrh,vzh:real):real;    {derivative to V of the relation
                                           between V and Load}

begin
    derfvcon := (3/2)*(1/(power(h,3)+6*h*vrh-12*vzh));
end;
{-----}
procedure Iteration;                  {Newton-Raphson iteration}

var controll1,control2,help1,help2 : real;

begin
    repeat
        controll1 := vrh(h_new[i,0]);
        control2 := vzh(h_new[i,0]);
        help1 := fvcon(V_old[i,0],h_new[i,0],Load[i,0],controll1,control2);
        help2 := derfvcon(h_new[i,0],controll1,control2);
        V_new[i,0] := V_old[i,0] - (help1/help2);
        h_new[i,0] := h_new[i-1,0] - (1/2)*(V_new[i-1,0]+V_new[i,0])*Time_Step;
        V_old[i,0] := V_new[i,0];
    until (fvcon(V_new[i,0],h_new[i,0],Load[i,0],controll1,control2) < crit);
end;

```

```

{-----}
      Main Program
{-----}

begin

      clrscr;
      Read_Input_File;
      Begin_Conditions;

      help0 := cosh(1/delta)           ;
      help1 := sinh(1/delta)          ;
      help2 := (eta*delta/beta)*(help0-1) ;
      help3 := (beta/delta)*help0     ;
      help4 := eta*help1              ;

      i      := 1;

      repeat
          V_old[i,0] := V_new[i-1,0];
          h_new[i,0] := h_new[i-1,0];
          Iteration;
          i:=i+1;
      until (h_new[i-1,0]<0) or (i-1>Number_Of_Timesteps);
      Counter:=i-2;
      Write_Output_File;
end.

{-----}

```


Appendix III Constraints on the constitutive relations for the mixture

Constitutive relations have to satisfy the conservation laws and the axiom of thermodynamics. Since the balance of both momentum and energy contain source terms, these equations can always be satisfied. Therefore constitutive relations are called admissible if conservation of mass and the second axiom of thermodynamics are satisfied.

The second axiom of thermodynamics, also called the entropy inequality, reads (Oomens 1985, page 3.17):

$$\begin{aligned}
 & -\rho^s \dot{\psi}^s - \rho^f \dot{\psi}^f - \rho^s \eta^s \dot{\theta}^s - \rho^f \eta^f \dot{\theta}^f + \\
 & + \sigma^s : D^s + \sigma^f : D^f - \bar{\pi}^s \cdot \bar{v}^s - \bar{\pi}^f \cdot \bar{v}^f + \\
 & - c^s (\psi^s + \frac{1}{2} \bar{v}^s \cdot \bar{v}^s) - c^f (\psi^f + \frac{1}{2} \bar{v}^f \cdot \bar{v}^f) + \\
 & + \frac{1}{\theta^s} \bar{h}^s \cdot \bar{\nabla} \theta^s + \frac{1}{\theta^f} \bar{h}^f \cdot \bar{\nabla} \theta^f \geq 0
 \end{aligned} \tag{III.1}$$

where:

$\frac{d}{dt}$ or $\dot{}$	material time derivative
ψ	specific Helmholtz free energy = $\phi - \theta\eta$
ϕ	specific internal energy
θ	absolute temperature
η	specific entropy
\bar{h}	heatflux vector

Note that by the entropy inequality, the internal entropy production for the mixture as a whole is always greater than or equal to zero, but that this is not necessarily required for each component separately.

assumption 10 The process is assumed to be isothermal, in other words, the absolute temperature θ is constant and equal for all constituents :

$$\frac{\partial \theta}{\partial t} = 0, \quad \vec{\nabla} \theta = \vec{0} \quad (\text{III.2})$$

Moreover the mass exchange due to chemical interaction is neglected (2.21) :

$$c^\alpha = 0 \quad (\text{III.3})$$

Now (III.1) becomes :

$$- \rho^s \dot{\psi}^s - \rho^f \dot{\psi}^f + \sigma^s : D^s + \sigma^f : D^f - \vec{\pi}^s \cdot \vec{v}^s - \vec{\pi}^f \cdot \vec{v}^f \geq 0 \quad (\text{III.4})$$

The balance of mass reads (2.24) :

$$\vec{\nabla} \cdot (\mathbf{n}^f (\vec{v}^f - \vec{v}^s)) + \vec{\nabla} \cdot \vec{v}^s = 0 \quad (\text{III.5})$$

The balance of mass is incorporated into the entropy inequality, multiplied by a Lagrange multiplier λ :

$$\begin{aligned} & - \rho^s \dot{\psi}^s - \rho^f \dot{\psi}^f + \sigma^s : D^s + \sigma^f : D^f + \\ & - \vec{\pi}^s \cdot \vec{v}^s - \vec{\pi}^f \cdot \vec{v}^f + \lambda (\vec{\nabla} \cdot (\mathbf{n}^f (\vec{v}^f - \vec{v}^s)) + \vec{\nabla} \cdot \vec{v}^s) \geq 0 \end{aligned} \quad (\text{III.6})$$

The dependent variables are $\psi^s, \psi^f, \sigma^s, \sigma^f$ and $\vec{\pi}^s$, ($\vec{\pi}^f = -\vec{\pi}^s$). The independent variables are chosen to be the deformation tensor for the solid \mathbf{F} , the density of the fluid ρ^f , the density gradient $\vec{\nabla} \rho^f$, and the relative velocity of the fluid with respect to the solid ($\vec{v}^f - \vec{v}^s$).

Inequality (III.6) now can be expressed as (Oomens 1985, page 3.22):

(III.7):

$$\begin{aligned}
& \left[-\rho^s \mathbf{F} \cdot \frac{\partial \psi^s}{\partial \mathbf{E}^s} \cdot \mathbf{F}^c - \rho^f \mathbf{F} \cdot \frac{\partial \psi^f}{\partial \mathbf{E}^s} \mathbf{F}^c + \sigma^s + \lambda n^s \mathbf{I} - \rho^s (\bar{v}^f - \bar{v}^s) \frac{\partial \psi^s}{\partial (\bar{v}^f - \bar{v}^s)} \right] : \mathbf{D}^s + \\
& + \left[(\rho^f)^2 \frac{\partial \psi^f}{\partial \rho^f} \mathbf{I} + \rho^f \rho^s \frac{\partial \psi^s}{\partial \rho^f} \mathbf{I} + \sigma^f + \lambda n^f \mathbf{I} + \rho^s (\bar{v}^f - \bar{v}^s) \frac{\partial \psi^s}{\partial (\bar{v}^f - \bar{v}^s)} \right] : \mathbf{D}^f + \\
& - \rho^f \frac{\partial \psi^f}{\partial \mathbf{E}^s} : (\bar{\nabla} \mathbf{E}^s \cdot (\bar{v}^f - \bar{v}^s)) + \\
& - \left(\rho^f \frac{\partial \psi^f}{\partial (\bar{\nabla} \rho^f)} + \rho^s \frac{\partial \psi^s}{\partial (\bar{\nabla} \rho^f)} \right) \cdot \frac{d^f(\bar{\nabla} \rho^f)}{dt} - \frac{\partial \psi^s}{\partial (\bar{\nabla} \rho^f)} \cdot (\bar{\nabla}^2 \rho^f \cdot (\bar{v}^f - \bar{v}^s)) + \\
& - \left(\rho^f \frac{\partial \psi^f}{\partial (\bar{v}^f - \bar{v}^s)} + \rho^s \frac{\partial \psi^s}{\partial (\bar{v}^f - \bar{v}^s)} \right) \frac{d^f(\bar{v}^f - \bar{v}^s)}{dt} + \\
& + \bar{\pi}^s \cdot (\bar{v}^f - \bar{v}^s) + \left[\frac{\lambda}{\rho^f} + \rho^f \frac{\partial \psi^s}{\partial \rho^f} \right] (\bar{v}^f - \bar{v}^s) \cdot \bar{\nabla} \rho^f \geq 0
\end{aligned}$$

assumption 11 Cartilage is assumed to be a 'simple' biphasic mixture, i.e., the Helmholtz free energy ψ^α of each phase does not depend on the properties of the other phase (Hou, 1989). Also the Helmholtz free energy for the fluid phase ψ^f does not depend on the fluid density ρ^f due to the negligible diffusion effect (Hou 1989, page 47-48).

assumption 12 Changes in the mixture's volume only arise from fluid flow into or out of the mixture, since the constituents are incompressible. Resulting changes in the volume fractions n^f and n^s will be neglected.

Now (III.7) becomes :

$$\left[-\rho^s \mathbf{F} \cdot \frac{\partial \psi^s}{\partial \mathbf{E}^s} \cdot \mathbf{F}^c + \boldsymbol{\sigma}^s + \lambda n^s \mathbf{I} \right] : \mathbf{D}^s + \left[\boldsymbol{\sigma}^f + \lambda n^f \mathbf{I} \right] : \mathbf{D}^f + \bar{\boldsymbol{\pi}}^s \cdot (\bar{\mathbf{v}}^f - \bar{\mathbf{v}}^s) \geq 0 \quad (\text{III.8})$$

The following constitutive relations satisfy the inequality shown above :

$$\boldsymbol{\sigma}^s = -\lambda n^s \mathbf{I} + \rho^s \mathbf{F} \cdot \frac{\partial \psi^s}{\partial \mathbf{E}^s} \cdot \mathbf{F}^c + \boldsymbol{\sigma}^{sv} \quad (\text{III.9})$$

$$\text{with } \boldsymbol{\sigma}^{sv} : \mathbf{D}^s \geq 0,$$

$$\boldsymbol{\sigma}^f = -\lambda n^f \mathbf{I} + \boldsymbol{\sigma}^{fv} \quad (\text{III.10})$$

$$\text{with } \boldsymbol{\sigma}^{fv} : \mathbf{D}^f \geq 0.$$

The tensor $\boldsymbol{\sigma}^{sv}$ represents the viscous part of the stress tensor $\boldsymbol{\sigma}^s$.

assumption 13 The cartilage is assumed to be a homogeneous, isotropic mixture of a purely elastic solid and a Newtonian viscous fluid.

Therefore the viscous part of the solid stress tensor equals zero :

$$\boldsymbol{\sigma}^{sv} = \mathbf{0} \quad (\text{III.11})$$

The Lagrange multiplier λ has to be interpreted as the hydrodynamic pressure p (Oomens 1985, page 3.23):

$$\lambda = p \quad (\text{III.12})$$

Note that also :

$$\vec{\pi}^s \cdot (\vec{v}^f - \vec{v}^s) \geq 0 \quad (\text{III.13})$$

The last restriction will be satisfied by the following relation for the body forces due to interaction ($\vec{\pi}^s = -\vec{\pi}^f$) :

$$\vec{\pi}^s = \mathbf{K} \cdot (\vec{v}^f - \vec{v}^s) \quad (\text{III.14})$$

where \mathbf{K} is a positive definite tensor, which for the isotropic case is $\mathbf{K} = K \mathbf{I}$ (Hou 1989, page 47). K is called the dragcoefficient.

Samenvatting

Het doel van dit rapport is het vergroten van het inzicht in squeeze film smering, een mechanisme dat verantwoordelijk wordt geacht voor de smering in de knie en dat mede tot stand komt als gevolg van de viscositeit van zowel de synoviaal vloeistof als de interstitiële vloeistof. Squeeze film smering is gebaseerd op het principe dat drukopbouw plaats vindt in een viskeuze vloeistoffilm die tussen twee loodrecht naderende oppervlakken wordt uitgeperst.

Drie verschillende squeeze films zijn onderzocht, namelijk een squeeze film tussen:

1. twee starre impermeabele cirkelvormige schijven
2. een starre impermeabele bolkop en een star impermeabel vlak
3. een starre impermeabele cirkelvormige schijf en een star permeabel mengsel

Voor elke situatie zijn de dikte van de squeeze film als functie van de tijd en de drukverdeling over de squeeze film berekend bij een gegeven belasting op de bovenste schijf of bolkop. Uit vergelijking van de tweede met de eerste situatie blijkt dat de drukverdeling opmerkelijk beïnvloed wordt door de geometrie van de squeeze film. Bovendien blijft de squeeze film in de tweede situatie veel korter in stand dan in de eerste situatie.

In de derde situatie wordt interactie tussen de squeeze film en de interstitiële vloeistof bereikt middels de randvoorwaarden die Hou in 1989 heeft afgeleid. Bovendien zijn voor deze situatie parameters gedefiniëerd die het mengsel karakteriseren. De invloed van de aanwezigheid van een star mengsel wordt duidelijk naar voren gebracht door vergelijking van de filmdikte als functie van de tijd voor verschillende parametersets.

Het is waardevol om in de toekomst de interface randvoorwaarden van Hou experimenteel te toetsen aan een fysisch squeeze film model waarin een mengsel is opgenomen.